Polymer 70 (2015) A17–A34

Contents lists available at ScienceDirect

Polymer

journal homepage: www.elsevier.com/locate/polymer

Feature article

Tailoring the interface in graphene/thermoset polymer composites: A critical review

Rani Rohini, Prajakta Katti, Suryasarathi Bose*

Department of Materials Engineering, Indian Institute of Science, Bangalore 560012, India

ARTICLE INFO

Article history:
Received 13 March 2015
Received in revised form
10 June 2015
Accepted 11 June 2015
Available online 15 June 2015

Keywords:
Graphene oxide
Thermoset polymers
Surface modification
Structure-properties

ABSTRACT

With the emergence of scientific interest in graphene oxide (GO) in recent times, researchers have endeavored to incorporate GO in thermoset polymeric matrix to develop composites with extraordinary set of properties. The current state of research in graphene/thermoset polymer composites is highlighted here with a focus on the role of interface in dictating the overall properties of the composites. Different strategies like covalent and non-covalent functionalization of GO have been discussed with respect to improvement in mechanical, electrical, thermal and rheological properties. In addition, future prospects have been outlined. By assessing the current state of research in graphene/thermoset composites, it is obvious that graphene derivatives are promising materials in enhancing the structural properties of the nanocomposites at extremely low levels of filler loading. This opens new avenues in designing light-weight composites for myriad applications and by tailoring the interfacial adhesion with the polymer, ordered structure can be achieved at macroscopic processing scales.

1. Introduction and background

Graphene, a 2-D monolayer sheet of several densely packed C-atoms with sp^2 hybridization has revolutionized the field of materials science. Theoretically, it was established in 1940 while, in 1962, Boehm was able to successfully extract thin carbon layers from graphite oxide. In 2004, successful preparation and isolation of stable graphene sheets by Nobel laureates Andre Geim and Konstantin Novoselvo led to the realization of outstanding properties of grapheme [1–3]. It showed extraordinary mechanical properties, electrical conductivity, thermal conductivity and optical transparency. Graphene is the source of all graphitic form or in other words, it is the building block (Fig. 1). Graphene in general is expensive compared to other carbon based nanofillers such as carbon nanotubes, nanofibers, etc. Though some of graphene derivatives, such as GO are inexpensive. Different graphene derivatives assist in manipulating the properties of a polymer in developing unique composites. Graphene, graphene nanoplatelets, graphene oxide (GO) and reduced graphene oxide have drawn considerable attention among the researchers owing to their widely different applications. Their highly competing properties such as mechanical stiffness (>1000 GPa), thermal conductivity (as high as 3000 $Wm^{-1} K^{-1}$), high charge mobility, high specific surface area (2600 m^2/g), high electrical conductivity of the order 2×10^3 S cm^{-1} and high thermal stability up to approx. 600 °C, etc. makes them ideal candidates for polymeric nanocomposites [3,4]. The potential applications range from solar cells, sensors, to drug delivery and bone replacements [5–13].

In this review article, the current state of research in graphene based thermoset polymers like epoxy, polyesters, and polyurethane-based composites are highlighted with an objective to provide a comprehensive overview on the structure-property correlationship in this field with a special attention to the role of interface in dictating the properties. The different strategies to synthesize GO and reduced GO, the different strategies to improve the interface with the polymer and the properties have been addressed with respect to the literature available from the last decade.

2. Different synthesis routes

There are different methods, which are being currently employed to synthesize layers of graphene and graphene oxide, such as chemical vapor deposition, mechanical processes, chemical reduction, unzipping of carbon nanotubes, organic synthesis route,

* Corresponding author.
E-mail address: sbose@materials.iisc.ernet.in (S. Bose).

http://dx.doi.org/10.1016/j.polymer.2015.06.016
0032-3861/

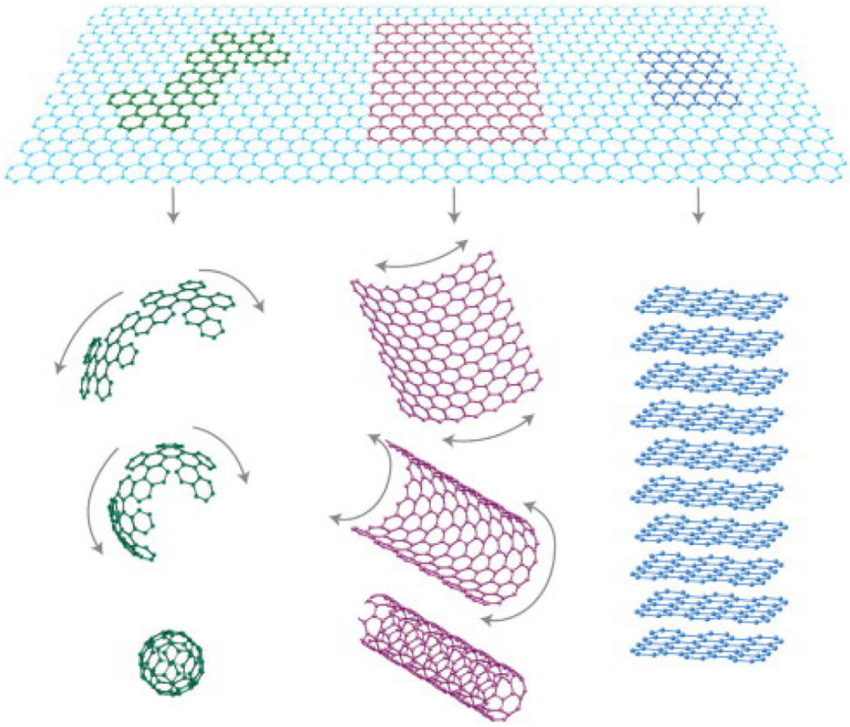

Fig. 1. Graphene as a building block of graphitic material. Reproduced by permission from Ref. [13]. Macmillan Publishers Ltd: [Nature], copyright (2007).

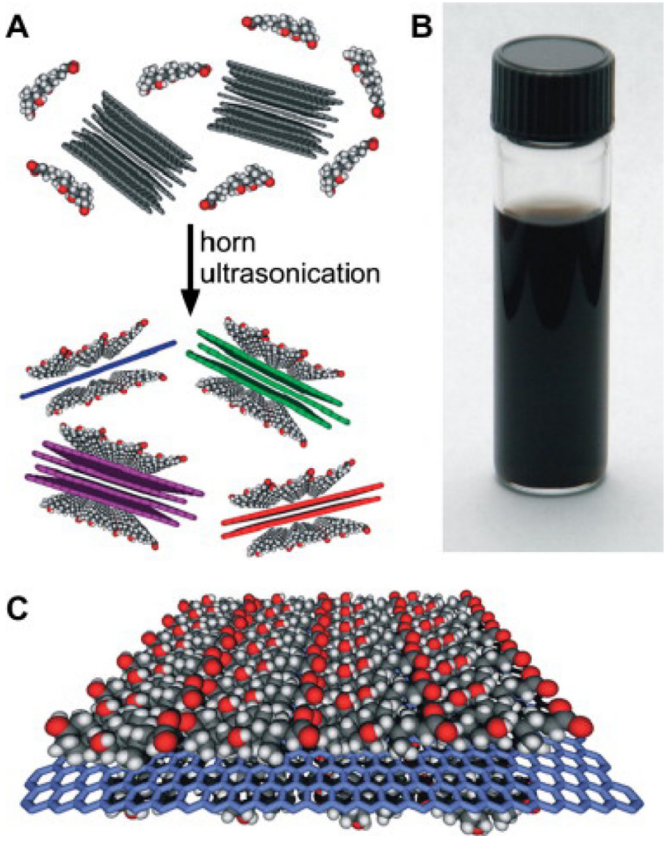

Fig. 2. (A) Schematic illustration of the graphene exfoliation process. Graphite flakes are combined with sodium cholate in aqueous solution. Horn ultrasonication exfoliates few-layer graphene flakes that are encapsulated by SC micelles. (B) Photograph of a 90 μg mL^{-1}graphene dispersion in SC six weeks after it was prepared. (C) Schematic illustrating an ordered SC monolayer on graphene. Reproduced by permission from Ref. [15]. Copyright© 2009 American Chemical Society.

etc. These synthesis techniques are divided depending on the application requisites, in other words, methods are either large or small scale based on purity and precision. Given the brevity of this review, here we will briefly discuss some of the regularly used techniques to synthesize GO and reduced GO and the commonly used characterization techniques to ascertain the reduction process.

2.1. Mechanical process

It involves exfoliation of graphene by different electrical and mechanical means; however, poor yield limits the usage of this technique. Later, researchers attempted to first chemically reduce graphite-to-graphite oxides and then subjected it to exfoliation. Some work in this area also involved exfoliation of graphite in water to produce graphene in presence of a surfactant like sodium dodecyl benzene sulfonate (SDBS). From Raman analysis, no D-band was observed in the spectrum suggesting a defect-free structure, which was further supported with HRTEM. Further electrical study showed reduced conductivity due to the presence of residual surfactant [14].

Efforts were also made to introduce small or guest molecules such as sodium cholate in between the graphite layers by exfoliation and later expanding these layers to prepare high quality graphene sheets (see Fig. 2.). It was found that on annealing at 250 °C sheet resistance of graphene decreased by the order of 2–4 and high optical transmittance was observed [15].

2.2. Chemical vapor deposition (CVD)

Li et al. [16] prepared graphene sheets on copper foils as substrates using a mixture of methane and hydrogen at 1000 °C. The structure was verified using SEM and TEM micrographs, which showed wrinkled structures (Fig. 3). Graphene sheets were also prepared using different surfaces like glass and Si. In another effort

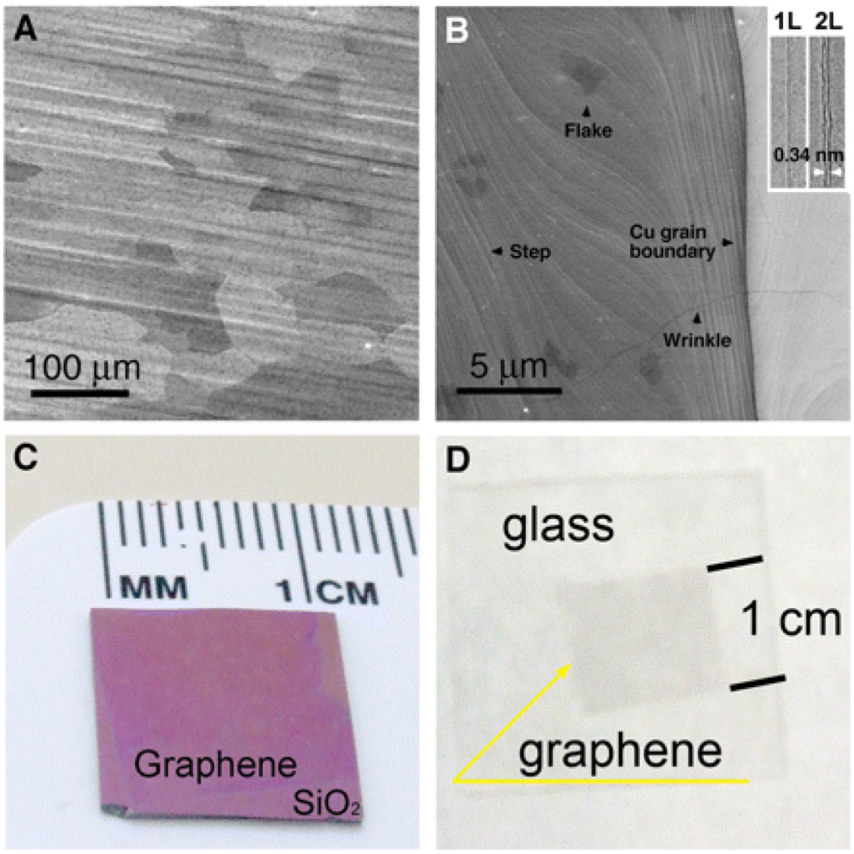

Fig. 3. (A) SEM image of graphene on a copper foil with a growth time of 30 min. (B) High-resolution SEM image showing a Cu grain boundary and steps, two- and three-layer graphene flakes, and graphene wrinkles. Inset in (B) shows TEM images of folded graphene edges. 1 L, one layer; 2 L, two layers. (C and D) Graphene films transferred onto a SiO_2/Si substrate and a glass plate, respectively. Reproduced by permission from Ref. [16]. Copyright© 2009 American Association for the Advancement of Science.

towards low cost graphene production, graphene sheets were grown on Ni films using CVD method. Carbon precipitates developed on the Ni surface during CVD process formed graphene layers over a larger area [17].

2.3. Unzipping of carbon nanotubes

CNTs were unzipped in order to obtain narrow graphene nanoribbons (GNR) with better structural control (Fig. 4). Structurally

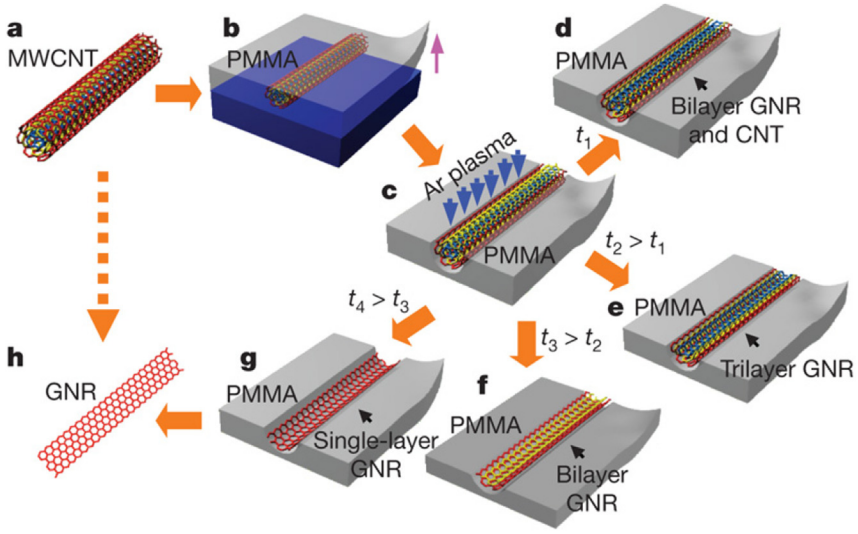

Fig. 4. a, A pristine MWCNT was used as the starting raw material. b, The MWCNT was deposited on a Si substrate and then coated with a PMMA film. c, The PMMA–MWCNT film was peeled from the Si substrate, turned over and then exposed to an Ar plasma. d–g, Several possible products were generated after etching for different times: GNRs with CNT cores were obtained after etching for a short time t1 (d); tri-, bi- and single-layer GNRs were produced after etching for times t2, t3 and t4, respectively (t4 > t3 > t2 > t1; e–g). h, The PMMA was removed to release the GNR. Reproduced by permission from Ref. [19]. Copyright 2009 Macmillan Publishers Ltd: [Nature].

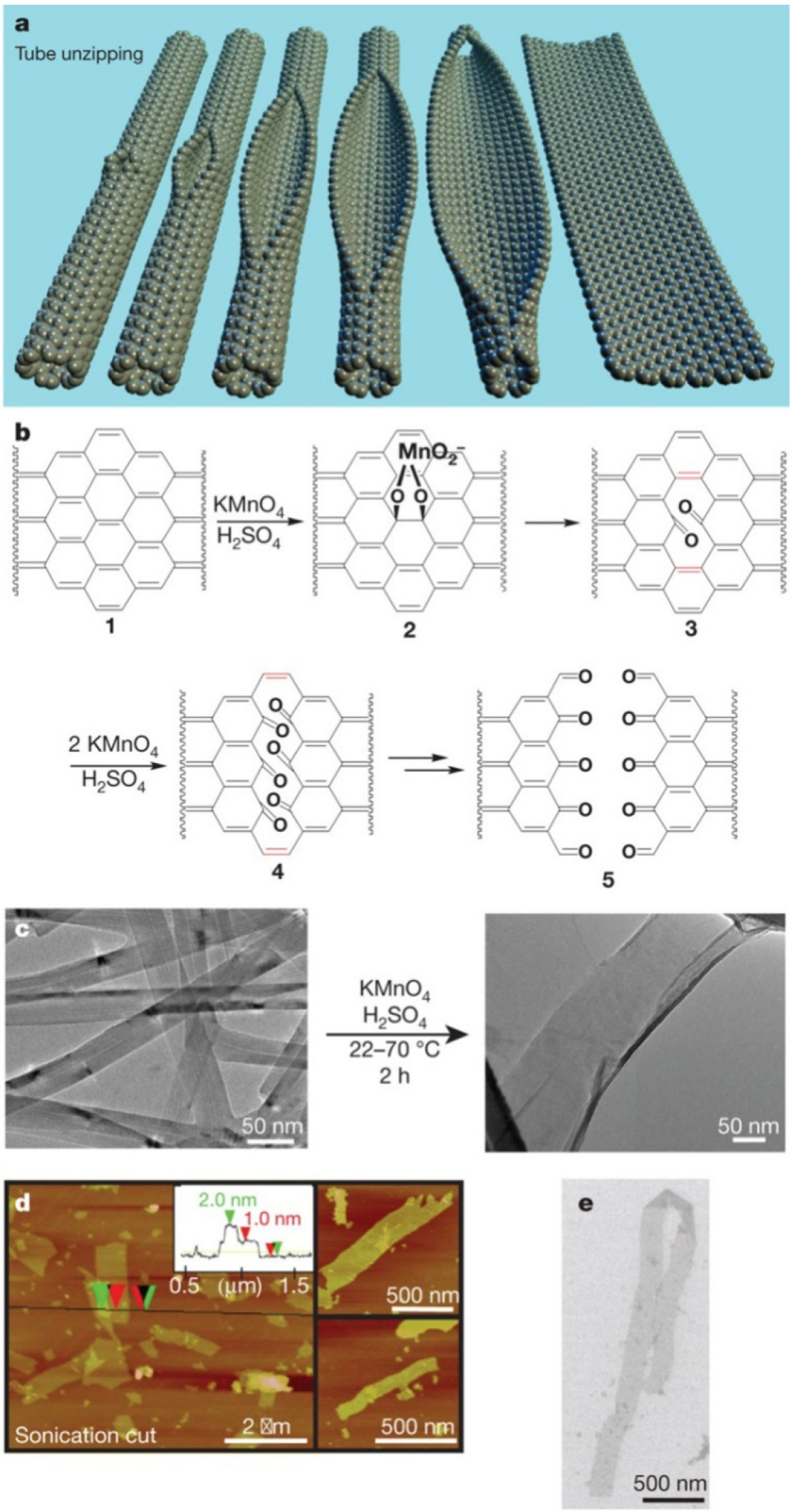

Fig. 5. a, Representation of the gradual unzipping of one wall of a carbon nanotube to form a nanoribbon. Oxygenated sites are not shown. b, The proposed chemical mechanism of nanotube unzipping. The manganate ester in 2 could also be protonated. c, TEM images depicting the transformation of MWCNTs (left) into oxidized nanoribbons (right). The right-hand side of the ribbon is partly folded onto itself. The dark structures are part of the carbon imaging grid. d, AFM images of partly stacked multiple short fragments of nanoribbons that were horizontally cut by tip-ultrasonic treatment of the original oxidation product to facilitate spin-casting onto the mica surface. The height data (inset) indicates that the ribbons are generally single layered. The two small images on the right show some other characteristic nanoribbons. e, SEM image of a folded, 4-μm-long single-layer nanoribbon on a silicon surface. Reproduced by permission from Ref. [20]. Copyright 2009 Macmillan Publishers Ltd: [Nature].

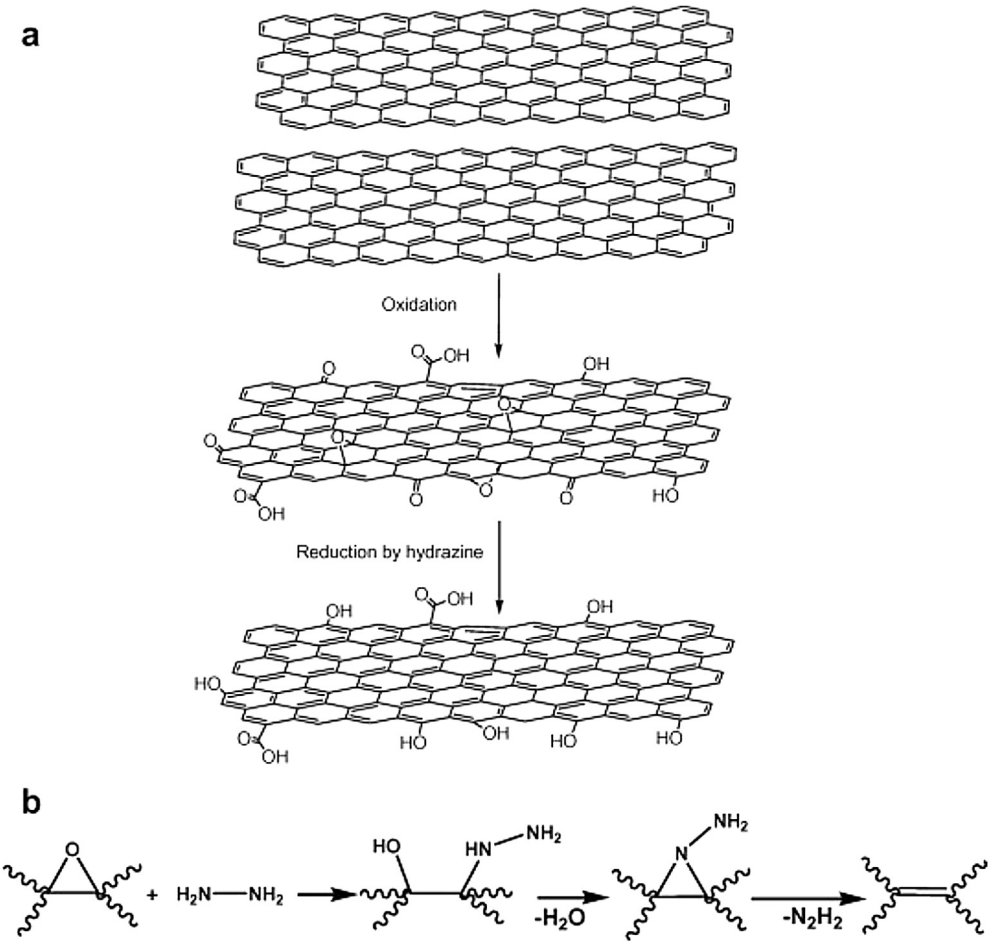

Fig. 6. (a) Oxidation of graphite to graphene oxide and reduction to reduced graphene oxide. (b) A proposed reaction pathway for epoxy reduction by hydrazine. Reproduced by permission from Refs. [1,22]. Copyright© 2011, 2007. Elsevier Ltd. All rights reserved.

controlled GNRs are of importance in electronic industries where precision is needed. Earlier methods to synthesize GNR based semiconductors using intercalation and exfoliation resulted in low yield and widely distributed size of ribbons, which is undesired [18]. In one of the recent studies, MWNTs of different diameters were embedded in PMMA on Si substrate, which was then etched with plasma for varied time scale. As a result, GNRs of different number of layers were obtained. PMMA was later dissolved in acetone, narrow sized GNRs were left out on the Si substrate [19].

In an attempt to fabricate nanoribbons through chemical route, Dmitry et al. [20] treated MWNTs in presence of concentrated H_2SO_4 followed by $KMnO_4$oxidation. The treatment was done for an hour at 22 °C and then at 55–70 °C for the same time, which resulted in nanoribbons and the cut, was either longitudinal or spiral depending on the initial site of attack. Nanoribbons were characterized by Transmission electron microscopy (TEM), Atomic force microscopy (AFM) and Scanning electron microscopy (SEM). The incremental effect of KMnO4 on the unzipping of MWCNTs was closely studied by TEM, X-Ray Diffraction (XRD) and ATR-Infrared spectroscopy (see Fig. 5).

2.4. Modified Hummers method

Above-mentioned methods were difficult to replicate at large scale. Back in 1957, Hummers proposed oxidation of graphite to prepare graphitic oxide. Later, this method was improved to synthesize graphene oxide on a larger scale and known as modified Hummers method originally proposed by Kovtyukhova et al., in 1999. The first step involves addition of concentrated H_2SO_4 to graphite flakes at ambient temperature. This mixture was then cooled and kept in ice bath; later $KMnO_4$ was added slowly and maintained at room temperature. Once the temperature of the mixture in the water bath reached 35 °C, it was then stirred for certain time, followed by cooling under ice bath. The purified water was added in excess. Hydrogen peroxide was then added until gas release from the mixture stops. Finally, synthesized graphene oxide was filtered, washed and purified using HCl solution. The obtained GO was then dried under vacuum [20]. Later in 2010 Marcanoet.al [21] presented a new method which involved further changes in modified Hummers methods. This method claims to be much simpler, high yield, better electrical conductivity and no release of toxic gas.

2.5. Chemically reduced graphene from graphite oxide

Typically, chemically reduced GO was obtained using hydrazine hydrate as shown in Fig. 6. In this method, the mixture of GO and H_2O were fed together and sonicated, until a clear brown homogeneous dispersion was obtained. To this solution hydrazine hydrate was then added followed by heating at 100 °C for 24 h, with water-cooled condenser attached to the round bottom flask. The precipitated black solid of reduced GO was obtained, which was then filtered and washed thoroughly with water and methanol. The product was then dried to obtain solid reduced GO [22].

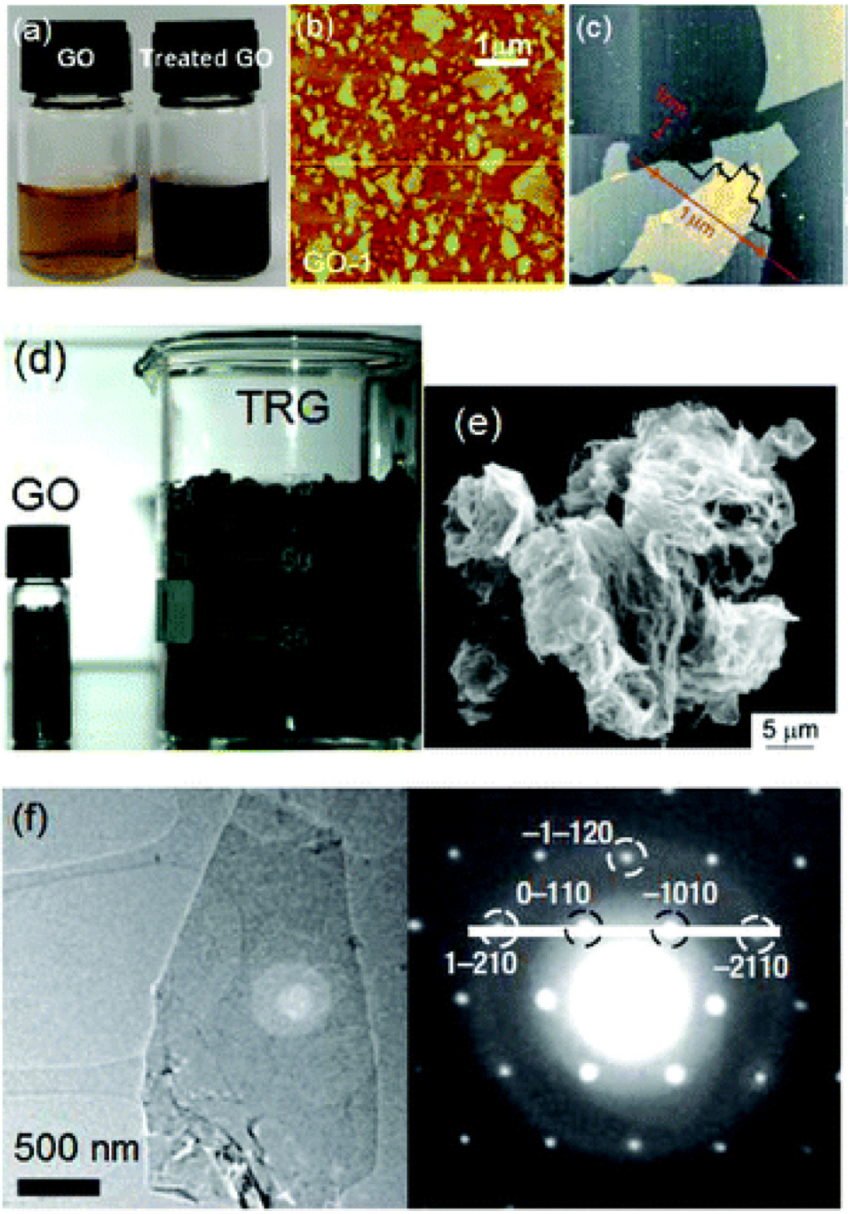

Fig. 7. (a) GO suspension (0.5–100/mL) before and after hydrothermal treatment at 180 °C; (b, c) noncontact mode AFM images of GO on mica; (d) 0.5 g of GO expands to 75 mL of TRG upon rapid heating to ~1000 °C; (e) SEM of TRG suggests a structure like crumpled sheets of paper, and (f) TEM image of a single-layer graphene with an electron diffraction pattern with Miller–Bravais indices. Reproduced by permission from Ref. [24]. Copyright© 2010, American Chemical Society.

2.6. Thermally reduced graphene from graphene oxide

Wufeng et al. [23] developed a simple and rapid method to reduce graphene oxide, thermally, to graphene using a microwave. In this method GO was dispersed in water and was sonicated with N,N-dimethylacetamide (DMAc) to obtain a clear yellow-brown suspension. Further, GO suspension was exposed to microwave for different time duration at 800 W. In the next stage, treated suspension was filtered and washed with ethanol to obtain a cake. Finally, black powder of graphene was collected. Fig. 7 show synthesis and characterization (AFM, TEM, SEM) of thermally reduced graphene oxide (TRG) [24].

3. Characterization

Commonly used techniques involved in characterizing graphene and GO are atomic force microscopy (AFM), optical microscopy, fluorescence quenching microscopy (FQM),transmission electron microscopy (TEM), scanning electron microscopy (SEM), Raman Spectroscopy. Optical Microscopy is one of the primary non-destructive technique to image graphene, GO and RGO layers. Samples are deposited on SiO_2 substrate to have better contrast. But has limited resolution and hence cannot image at small scale. FQM is another low cost technique which helps to analyze and optimize synthesis method in a short time period. The emission from dye coated samples is quenched to obtain micrographs. The contrast depends on the chemical interaction of dye with GO. AFM is used as an effective tool to image topography and layer thickness of graphene and GO. In some of the studies AFM has been used to understand the mechanical behavior of graphene under deformation. AFM microscopy usage is limited to the surface roughness of the sample. Graphene and RGO ultra-thin samples are viewed under TEM to study their atomic structure, as it provides atomic scale resolution. Raman spectroscopy helps

Table 1
Literature summary of graphene/thermoset composites.

Reinforcement	Modification	Covalent/non-covalent	Matrix	Remarks	Ref.
0.1 wt% functionalized graphene[a]	DBU/diethylbromomalonate	Covalent	Epoxy	18% ↑ in storage modulus 22% ↑ in flexural strength	[53]
5 wt% as prepared GO[a]			Epoxy	11% ↑ in tensile strength 24%↑ in tensile modulus	[38]
0.1 wt% graphene oxide[a]			Epoxy	75% ↑ in fracture toughness	[37]
1.5 wt% reduced graphene oxide[a]			Epoxy	55% ↑ in tensile strength 70% ↑ in tensile modulus	[69]
0.2 wt% amino functionalized GO[a]	APTS	Covalent	Epoxy	16% ↑ in tensile strength 32% ↑ in tensile modulus	[36]
0.1 wt% triton-graphene[a,b]	Non-ionic surfactant of Triton X-100	Non-covalent	Epoxy	57% ↑ in tensile strength	[62]
0.125 wt% functionalized graphene sheet[a]			Epoxy	45% ↑ in tensile strength 50% ↑ in Youngs modulus 65% ↑ in fracture toughness	[71]
0.1 wt% graphene platelets[a]			Epoxy	40% ↑ in tensile strength 31% ↑ in Youngs modulus 53%↑ in fracture toughness	[72]
0.0375 wt% graphene oxide[a]	Two-phase extraction		Epoxy	1185.2% ↑ in fracture toughness 48.3% ↑ in compressive strength	[39]
0.2 wt% graphene oxide[a]	DER332, DDM	Covalent	Epoxy	30% ↑ in tensile strength 62% ↑ in storage modulus 26 °C ↑ in T_g	[54]
2 wt% graphene oxide[a]	Hexachlorocyc-lotriphosphazene and glycidol	Covalent	Epoxy	113% ↑ in storage modulus	[55]
0.1 wt% graphene oxide[a]	APTES functionalized silica nanoparticles	Covalent	Epoxy	57% ↑ in fracture toughness at CT 53.5% ↑ in impact strength	[56]
1 wt% graphene oxide[a]	PU, epoxy	Covalent	Epoxy and polyurethane	50% ↑ in fracture toughness	[58]
0.25 wt% graphene oxide[a]	Microwave exfoliated, TETA	Covalent	Epoxy	45%↑ in tensile strength 50% ↑ in Youngs modulus 65% ↑ in fracture toughness	[70]
0.1 wt% graphene foam[e]	Layered surface		Epoxy	70% ↑ in fracture toughness	[73]
4 wt% grapheme nanosheets[a]	Py-PGMA–GNS	Non covalent	Epoxy	20% ↑ in thermal conductivity	[63]
0.5 wt% graphte nanoparticles[a]			Epoxy	50%↑ in Young's modulus ↑ in electrical conductivity by 5order	[59]
1 wt% grapheme nanosheets[a]	APTS	Covalent	Epoxy	45% ↑ in tensile strength 20 °C ↑ in T_g	[59]
Graphene oxide/PU[a]			Polyurethane	53% ↑ in fracture toughness	[74]
0.50 wt% D230-f-GO[b]	Polyether amine	Covalent	Polyether amine	63% ↑ in ultimate tensile strength 12 ↑ in elastic modulus 90% ↑ in fracture toughness	[60]
10 wt% SiO_2–GO[c,a]		Covalent	Epoxy	22.1% ↑ in tensile strength 8.5% ↑ in Youngs modulus 45.3% ↑ in fracture toughness 20 °C↑ in T_g	[65]
0.5 wt% SATPGO[a]		Covalent	Epoxy	154% ↑ in impact strength at RT 92% ↑ in impact strength at RT	[75]
3 wt% Al–GO[a]		Covalent	Epoxy	36.4% ↑ in storage modulus 20 °C↑ in T_g	[57]
0.1 wt% GO[a]			Epoxy	50% ↑ in fracture toughness	[76]
0.5 wt% GO[a]			Epoxy	35% ↑ in elastic modulus	[76]
0.08 wt% FGS (functionalized graphene sheets)[a]	Unsaturated polyester		Unsaturated polyester	53.6% ↑ in tensile strength 48.4% ↑ in tensile modulus	[77]
0.32 wt% FGS (functionalized graphene sheets)[a]	Unsaturated polyester	Covalent	Unsaturated polyester	10.7 °C ↑ in thermal decomposition temperature 17.9 °C ↑ in T_g	[77]
0.05 wt% GO[a]			Epoxy	36 °C ↑ in damping factor	[78]
1.6 wt% functionalized grapheme nanosheet[a]		Covalent	Epoxy	30–80% ↑ in fracture toughness at RT 200–700% ↑ in fracture toughness (−30 °C)	[67]
3 wt% rGO[a]			Unsaturated polyester	123% ↑ in tensile strength 87% ↑ in Young's modulus	[45]
0.05 wt% of GO sheets[a]		Covalent	Unsaturated polyester	72.2% ↑ in tensile strength	[79]
1.45 vol% graphene[a]		Covalent	Bio-based polyester	185% ↑ in thermal conductivity	[80]
3 wt% aqueous reduced graphene[a]			Thermoplastic polyurethane	568% ↑ in elastic modulus	[44]
5.0 wt% RGO[a]			Polyurethane	129% ↑ in elastic modulus	[43]
0.1 wt% graphene nanoplatelets[d]	Amine functionalization	Covalent	Epoxy	66% ↑ in fracture toughness	[81]
1 wt% expanded graphite (EG)[d,a]		Covalent	Epoxy	15% ↑ in elastic modulus	[82]
2 wt% graphenenanoplatelets (GnPs)[a,d]		Non covalent	Epoxy	82% ↑ in fracture toughness	[52]
≤1 wt% graphene oxide[d]			Epoxy	28–111% ↑ in mode I fracture toughness, 1580% ↑ in uniaxial tensile fatigue life	[83]

[a] Mechanical mixing.
[b] Ball milling.
[c] Shear mixing.
[d] Three roll milling.
[e] Others.

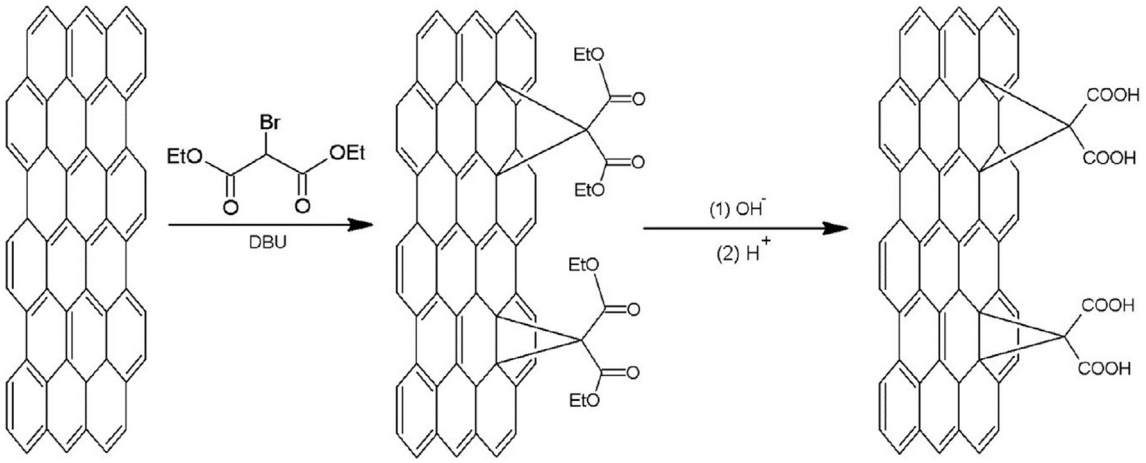

Fig. 8. Synthesis of functionalized graphene via bingel reaction. Reproduced by permission from Ref. [53]. Copyright 2014 Macmillan Publishers Ltd: [Nature].

to identify number of layers, defects, effect of strain and doping concentration from intensity of G, D, 2D peaks of graphene, GO and RGO [1]. SEM is used to perform structural analysis of graphene films [25].

4. Graphene based polymer nanocomposites

Since its discovery, graphene has been viewed as a potential candidate to reinforce polymer matrices for wide range of applications in structures, automotive, packaging, aerospace, fire safety, filtration, electronics, electromagnetic interference (EMI) shielding, etc. [24,26–35] Graphene/polymer nanocomposites were processed using different processing technique i.e. melt mixing, solution mixing, in-situ polymerization and/or combination of them [24]. Significant enhancement in properties has been observed by addition of graphene-based particles [36–40]. GO with epoxide, carboxyl or hydroxyl functional groups assist in dispersion in the polymer matrix. In a review work Potts et al. [41] have described different derivatives of GO fillers based composites showing high electrical conductivity, high moduli, and ease of functionalization for desired applications.

Though graphene possesses extraordinary properties and has wide application capability, there is a need for functionalization of graphene. It has zero band-gap, shows inertness towards reactions and very less interaction with the polymer matrix. These behaviors of graphene restrict its applications to a certain extent. Functionalization of graphene is of great importance in dispersing and processing at macroscopic scale. Significant work on functionalization of graphene has been carried out for better properties. GO is the main source of graphene production. Hence functionalization of GO in order to reduce it to prepare graphene is a commonly used technique [42–45]. Therefore surface modification of GO is carried out by either covalent or non-covalent functionalization [2].

5. Graphene-thermoset nanocomposites

This following section of this review highlights the studies that have been carried out to improve critical parameters like dispersion and interfacial bonding of graphene and GO with the epoxy matrix [46–52]. GO has been functionalized with molecules and macromolecules covalently or non-covalently depending on the application. Covalent functionalization involves formation of a strong chemical bond between graphene and polymer, while non-covalent functionalization involves physical interaction and does not induce defects sites unlike covalent modification. Here, it will be discussed

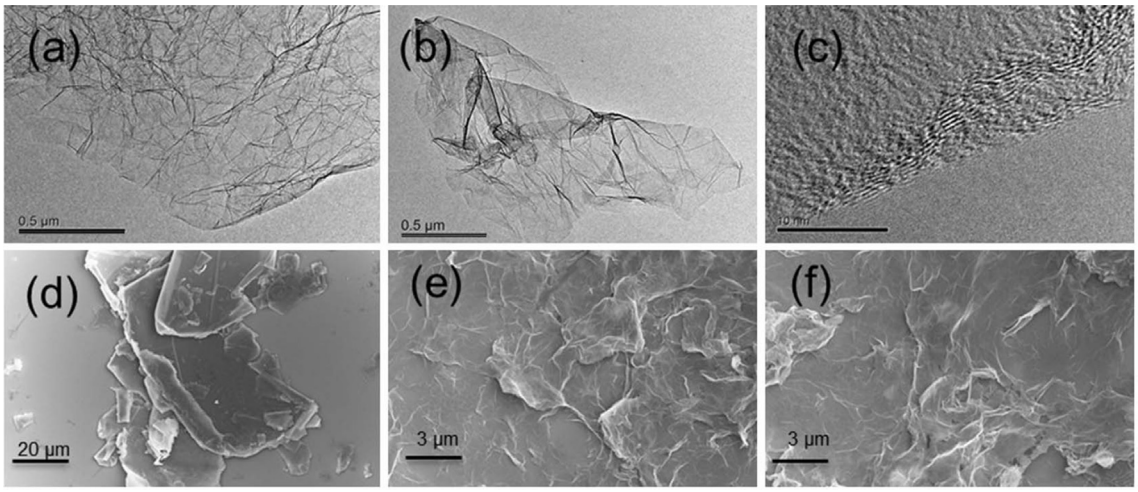

Fig. 9. Micrographs of TEM images of (a & c) TRG and (b) FG; SEM images of (d) natural flake graphite, (e) TRG and (f) FG. Reproduced by permission from Ref. [53]. Copyright 2014 Macmillan Publishers Ltd: [Nature].

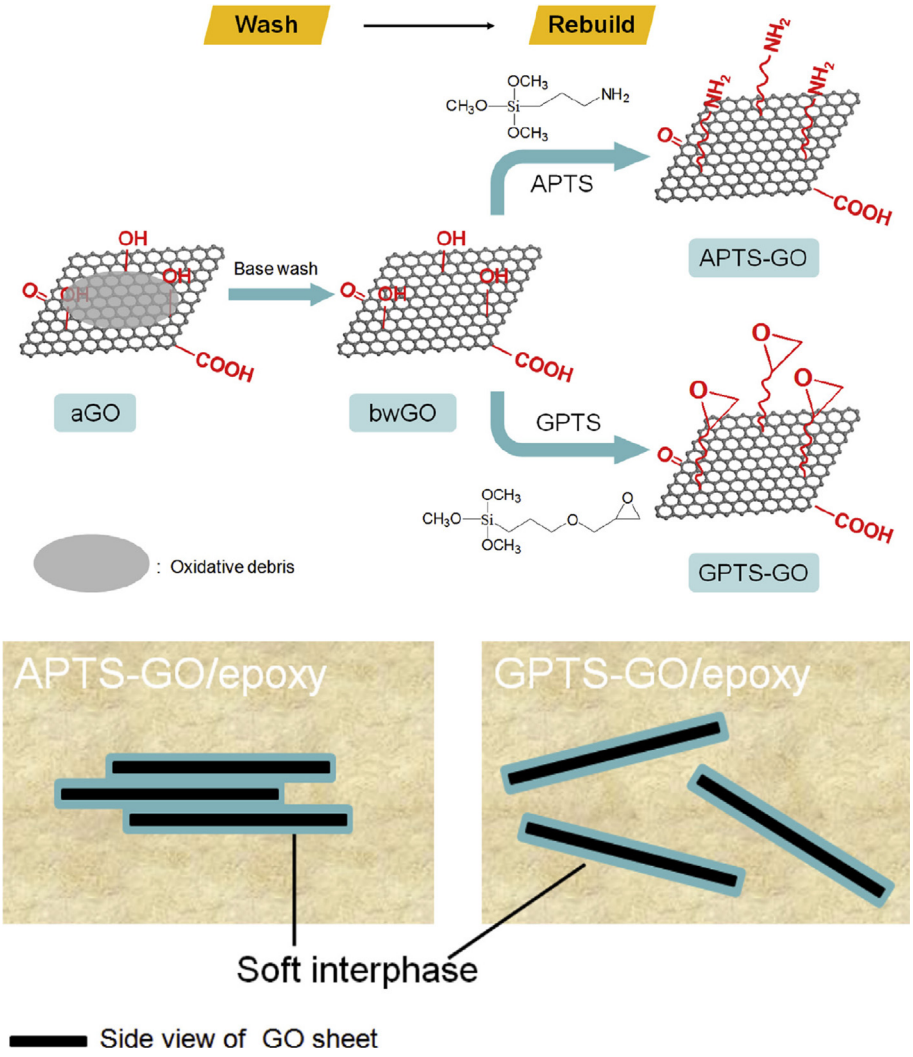

Fig. 10. Schematic illustration of the "wash-and-rebuild" process and the soft interphase in the modified GO/epoxy composite. Reproduced by permission from Ref. [36]. Copyright© 2013 Elsevier Ltd. All rights reserved.

different functionalization of GO adopted to improve the mechanical, electrical and thermal properties of epoxy based composites Table 1.

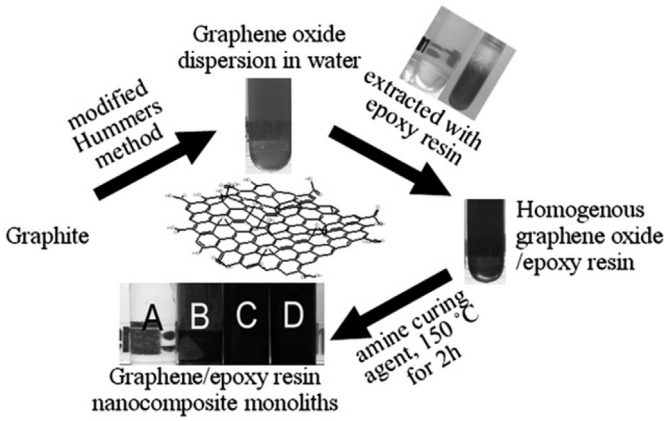

Fig. 11. Procedures to create the chemically converted graphene oxide/epoxy nanocomposite monoliths. Reproduced by permission from Ref. [39]. Copyright 2009 The Royal Society of Chemistry.

5.1. Covalent functionalization

Minoo et al. [53] described functionalization of GO with mixture of 1,8-diazabicycloundecene (DBU) and diethylbromomalonate, namely Bingel reaction, to study mechanical properties of epoxy composites. GO was synthesized using Hummers method and dried at 80 °C for 24 h under vacuum. GO was kept in a quartz tube in Ar atmosphere for 10 min, then thermally reduced in a Lindberg tube at 1050 °C in the furnace for 30 s. Reduced GO was named as TRG (thermally reduced graphene), which was further functionalized with mixture of 1,8-diazabicycloundecene (DBU) and diethylbromomalonate for 15 h in an inert atmosphere as shown in Fig. 8. The Fig. 9 shows TEM micrographs of functionalized GO and SEM micrographs of the composites. The functionalized graphene (FG) obtained was thoroughly filtered and washed. The epoxy composites were prepared by dispersing graphene in acetone. Composites were prepared with only 0.1 wt% of filler. The composites were subjected to mechanical loadings to study the flexural properties, storage modulus and glass transition using dynamic mechanical analyzer. Flexural strength was improved by 22% and 15% respectively for FG (0.1 wt%) and TRG (0.1 wt%) based epoxy nanocomposites compared to neat epoxy. Storage modulus was increased by 18% and 10% respectively for FG (0.1 wt%) and TRG (0.1 wt%)

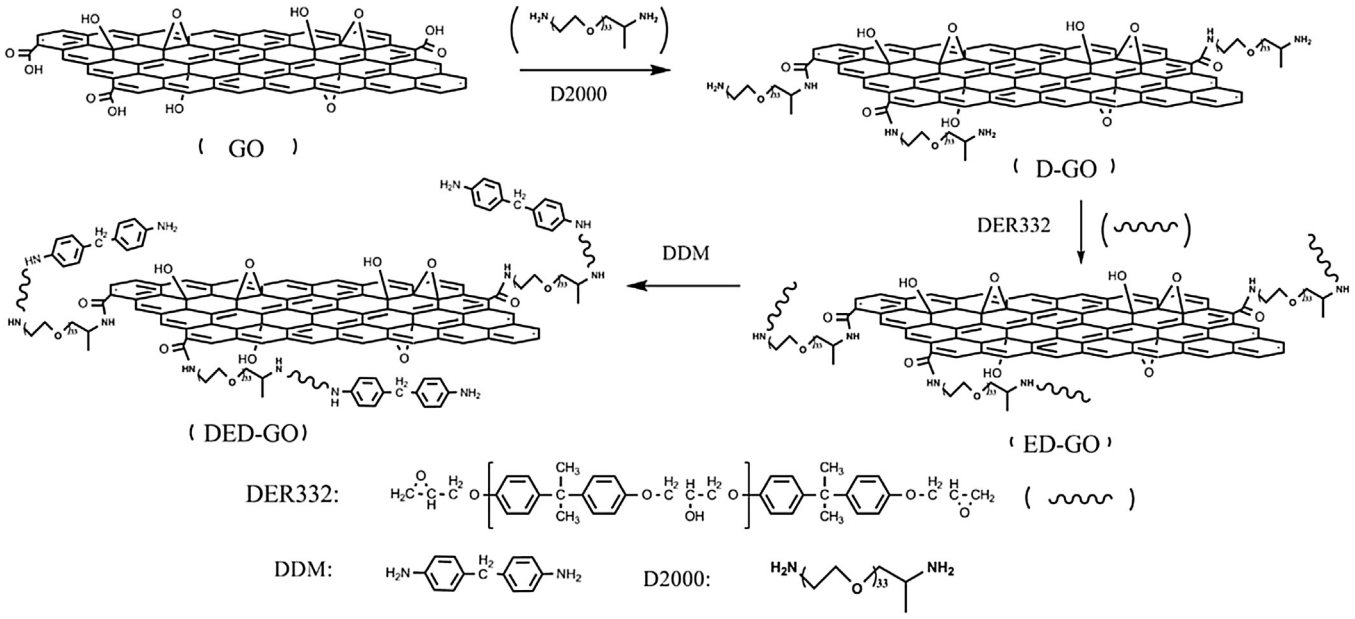

Fig. 12. Representation of reaction involved in grafting epoxy monomer and curing agents onto GO surface. Reproduced by permission from Ref. [54]. Copyright© 2014 Wiley Ltd. All rights reserved.

based epoxy nanocomposites. This increment was observed due to better dispersion and strong interfacial bonding [53].

In another study, GO was functionalized using 3-amin opropyltrimethoxysilane (APTS) and 3-glycidoxypropyltrimetho xysilane (GPTS) to improve the tensile strength and fracture toughness in epoxy nanocomposites and to understand different behavior of composites in presence APTS and GPTS. Epoxide group on GPTS favors better compatibility with epoxy matrix compare to

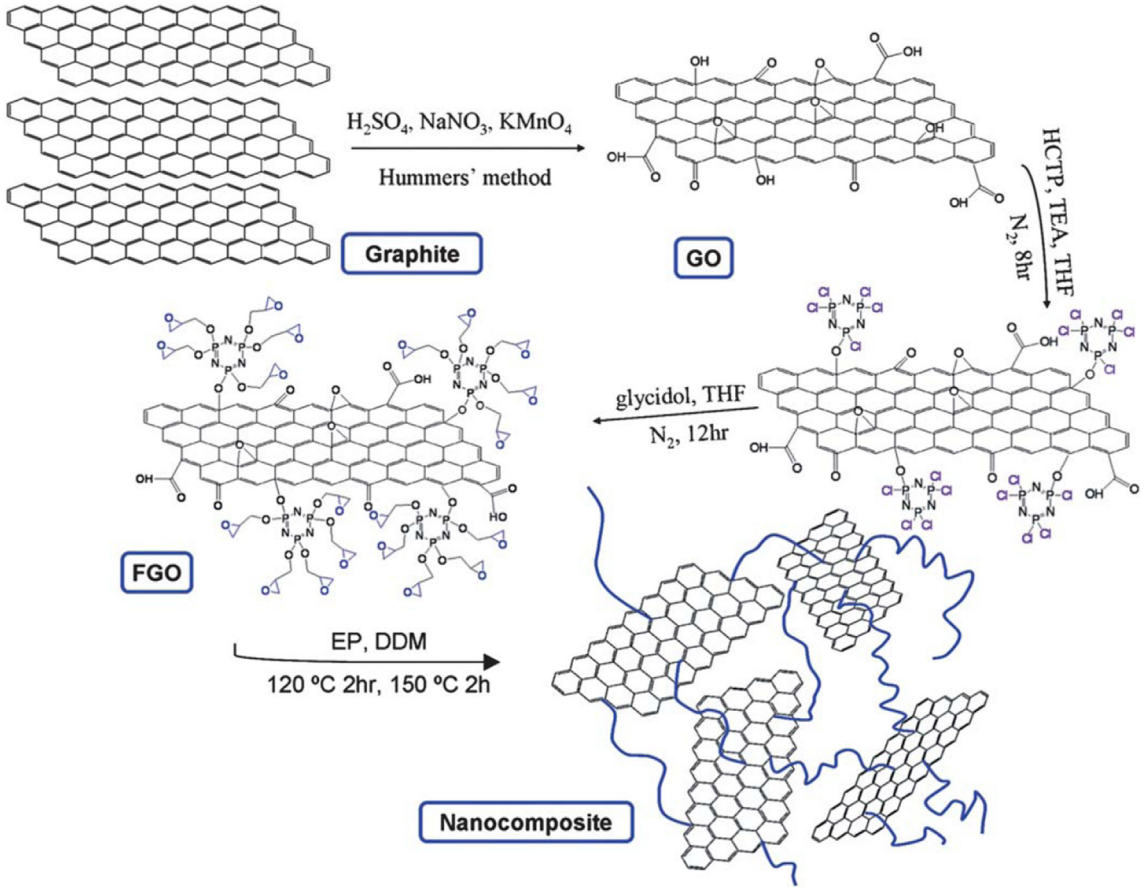

Fig. 13. Preparation route FGO and FGO/epoxy nanocomposites. Reproduced by permission from Ref. [55]. Copyright 2011 The Royal Society of Chemistry.

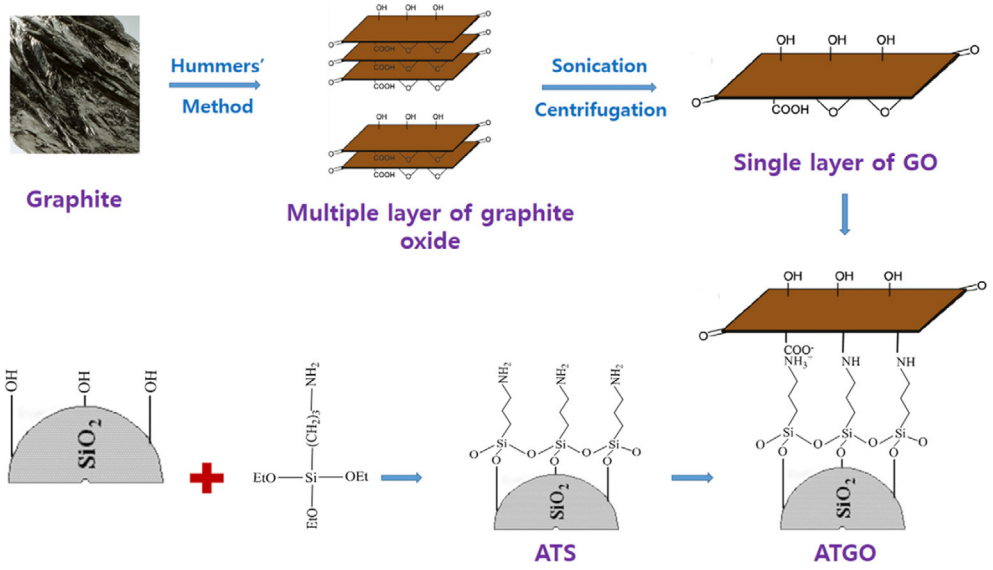

Fig. 14. Schematic for the preparation of GO, ATS, and ATGO. Reproduced by permission from Ref. [56]. Copyright© 2013 Elsevier Ltd. All rights reserved.

APTS. At a very low loading of APTS-GO of 0.2 wt%, the Young's modulus improved by 32% and tensile strength by 16%.This enhancement in properties can be attributed to efficient load transfer ability from matrix to GO. While fracture toughness and fracture energy of 0.2 wt% of GPTS–GO/epoxy nanocomposites doubled. This can be explained from the fact that formation of the soft interface around GO facilitates enhanced ductility to the matrix. Fig. 10 depicts schematic representation of functionalization of GO using "wash and build" method and shows soft interface between GO and matrix [36].

Chemically converted graphene oxide/epoxy nanocomposites were prepared using two-phase extraction method. Nanocomposite precursor with 0.0375 wt% loading were prepared and mechanical properties under compressive forces was studied (Fig. 11). It showed extremely high performance under compressive load. The compressive failure strength and toughness was improved by 48.3 and 1185.2% resp. This behavior shown can be explained by distortions occurred due to oxygen functionalization which led to emergence of defects in the nanocomposites. Hence increased surface roughness provided better interlocking of polymer chains and GO particles. Further presence of pendant groups on the GO surface formed covalent bond with epoxy resin which resulted in better interactions between filler and matrix [39].

Tinaxi et al. [54] prepared GO functionalized with epoxy and a curing agent (DED–GO), for homogeneous dispersion in epoxy resin, and also for universal applications of epoxy nanocomposites. Covalent functionalization of epoxy and curing agent diaminodiphenyl methane (DDM) on GO was carried out in three step method (see Fig. 12). Modified GO was dispersed in dichloromethane (DCM). The dispersed DED–GO was mixed with epoxy resin and mixed using magnetic stirrer for 10 min. Hardener was added after the removal of solvent followed by degassing and nanocomposites were cured in PTFE mold.

The mechanical and thermal analysis of DED–GO/epoxy nanocomposites at low filler loading showed enhanced properties. The nanocomposite with 0.1 wt% of DED–GO displayed an increment in T_g by 26 °C while 0.2 wt% showed 32% and 62% enhancement in tensile strength and storage modulus, and 18% increase in elongation at break respectively.

In a recent work by Chenlu et al. [55]. GO was surface modified with hexachlorocyclotriphosphazene (HCTP) and glycidol to prepare functionalized graphene oxide (FGO). FGO was later added to the epoxy resin followed by in-situ polymerization (see Fig. 13). FGO showed better dispersion in the matrix and resulted in improved "particle-matrix-particle" load transfer mechanism. The electrical conductivity showed a jump of more than 6 orders of magnitude at 5 wt% of FGO loading and, hardness and storage modulus was increased by 38% and 113% at 4 wt% and 2 wt% loading of FGO resp. was reported.

The toughening effect of functionalized GO on epoxy matrix was studied under cryogenic conditions. Silica particles were preferred for functionalization since it has polar–polar interaction with

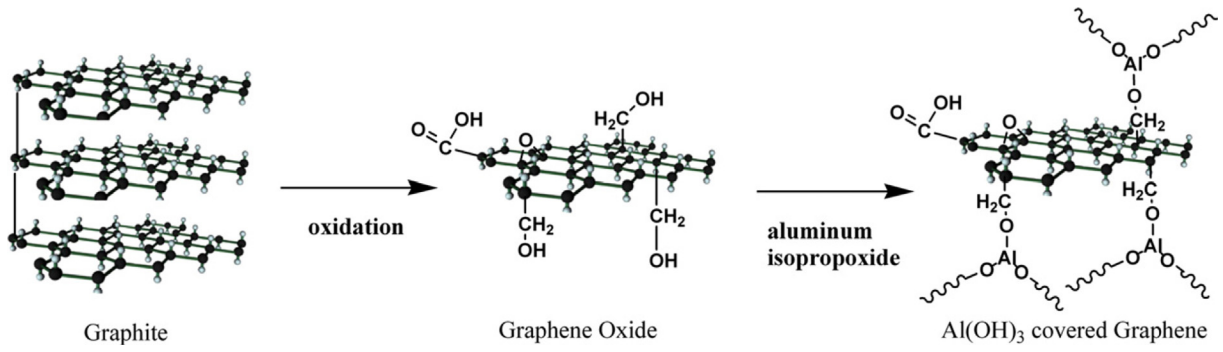

Fig. 15. Preparation of modified $Al(OH)_3$-coated GO composite. Reproduced by permission from Ref. [57]. Copyright© 2012 Elsevier Ltd. All rights reserved.

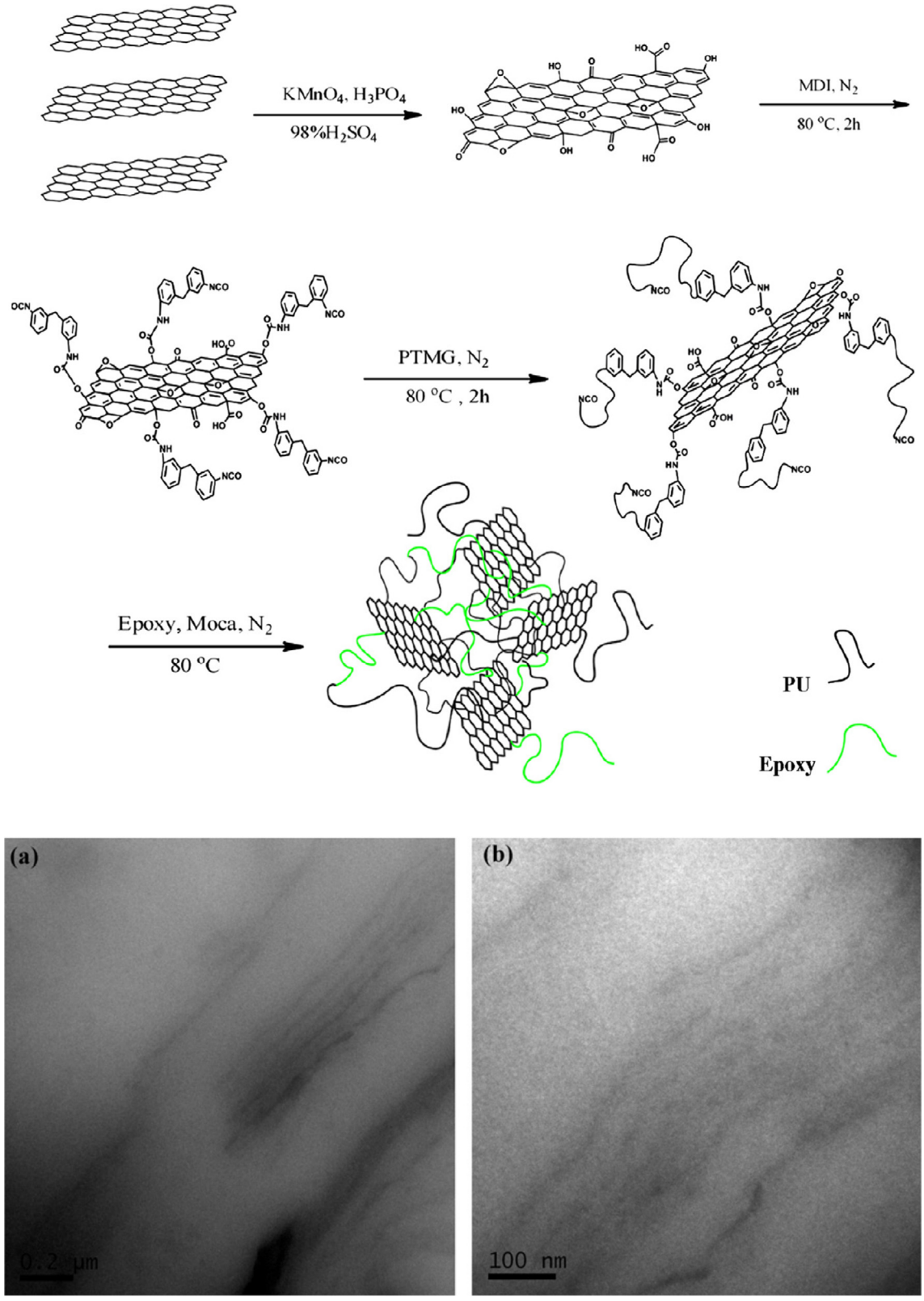

Fig. 16. Synthesis route of PU/GO/EP nanocomposites and TEM images of the PU/GO/EP nanocomposites: (a) PGE-1 (at low magnification) and (b) PGE-1 (at high magnification). Reproduced by permission from Ref. [58]. Copyright© 2013 Elsevier Ltd. All rights reserved.

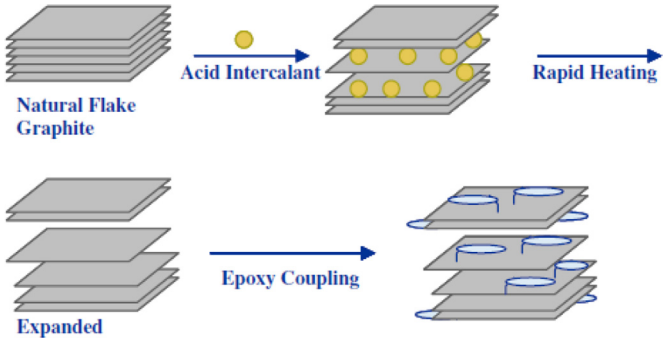

Fig. 17. Schematic of graphite expansion and functionalization process. Reproduced by permission from Ref. [40]. Copyright© 2010 Elsevier Ltd. All rights reserved.

epoxy matrix. 3-aminopropyltriethoxysilane (APTES) functionalized silica nanoparticles were synthesized and later covalently attached to the GO surface, namely, ATGO. Fig. 14 schematically represents the covalent functionalization of GO with silanized silica using a simple method. Further, mechanical properties were investigated by incorporating ATGO in epoxy matrix at different filler loading in the range of 0–3 wt% at room temperature and cryogenic temperature. The mechanical behavior shown by the composites were different at cryogenic temperature compared to ambient conditions. Single edge notched bending test provided fracture toughness of the samples and it was found to increase upto 1 wt% of the ATGO. It is envisaged that ATGO provided rough surface as revealed from SEM which allowed good dispersion and hence mechanical properties were enhanced [56].

GO was functionalized with aluminum isopropoxide to fabricate epoxy composites for adhesives application with better mechanical and thermal properties. The hydrolyzed aluminum isopropoxide was mixed with GO in methanol/DI water solution. Followed by hydrolysis, condensation reactions were carried out at 60 °C for 6 h. The final product was obtained after filtration and vacuum dried at 100 °C (Fig. 15). $Al(OH)_3$ covered GO showed even distribution in epoxy matrix and was characterized for hybrid interconnection test [57].

Yuki et al. [58] presented a facile method to prepare GO/Polyurethane (PU)/epoxy nanocomposites with enhanced mechanical and thermal properties. PU was polymerized in situ with GO (0.033 wt%) nanosheets. GO was sonicated in DMF and MDI was added at 80 °C for 2 h under N_2 condition. Later, Poly tetramethylene glycol (PTMG) was mixed under same condition, thus in situ polymerization was initiated. To this mixture epoxy and curing agent were introduced and stirred at 80 °C under vacuum until the mixture thickens. It was then poured and cured in a teflon mold. The TEM micrographs of the composite reveal good bonding of GO sheets with PU and epoxy (see Fig. 16).

Sandi et al. [40] proposed functionalization of graphite with epoxy resin with minimal damage to sp^2 hybridization and hence, retaining its inherent properties. It was evident from the mechanical and electrical properties of the epoxy composites. Functionalized graphite was synthesized as shown in Fig. 17 and was named as ATI graphite. With low loading of 0.5 wt%, electrical conductivity showed a jump of 5 orders, i.e., 2.2×10^6 Ohm cm, compared to neat epoxy samples, while unfunctionalized graphite showed 3×10^{10} Ohm cm. In addition mechanical properties such as strength and Young's modulus were improved due to the greater interfacial interactions of fillers and matrix however, ductility and toughness was reduced.

Benefiting from the multiple functional groups present on the silane coupling agents, graphene nanosheets (GNS) was covalently functionalized with 3-aminopropyltriethoxysilane (APTS) (see Fig. 18) which can act as a bridging agent between filler and matrix. 1 wt% f-GNS/epoxy composites displayed strong covalent interaction due to the presence of functional groups on f-GNS [59].

Li et al. [60] studied the effect of functionalization of GO on epoxy matrix by introducing different molecular weights of Polyetheramine (PEA) to obtain superior performance (see Fig. 19). The presence of amine functional groups on PEA functionalized GO assisted in copolymerization with epoxy resin and hence improved the interfacial adhesion. PEA-f-GO/epoxy composites formed soft

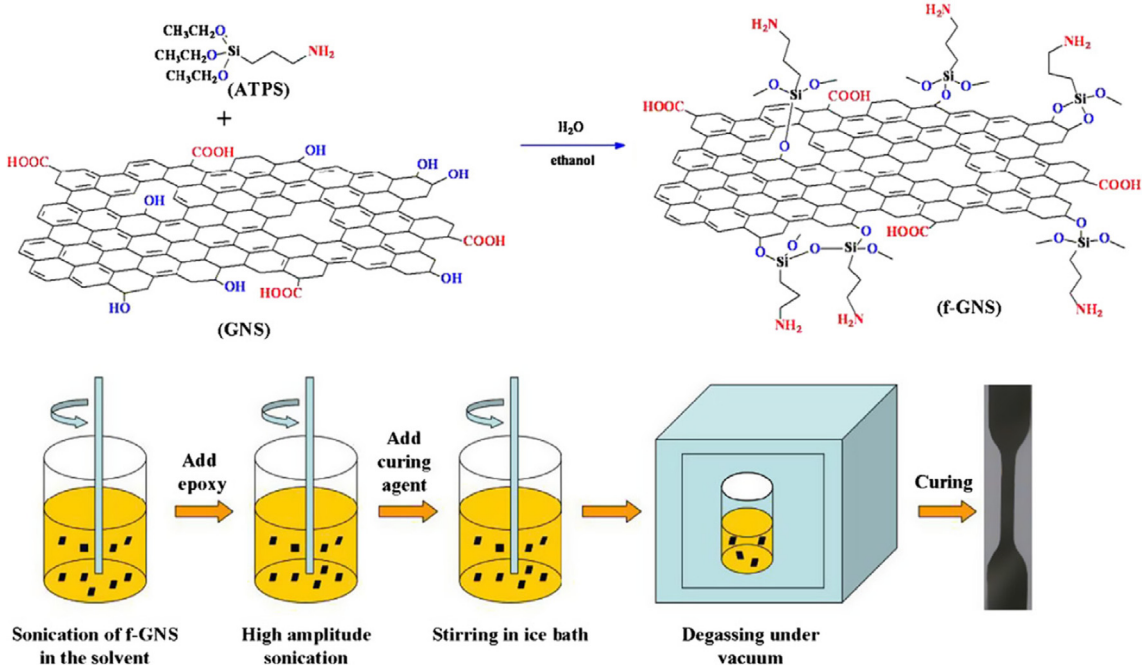

Fig. 18. Illustration of the reaction between GNS and APTS, and incorporation of f-GNS sheets into the epoxy matrix. Reproduced by permission from Ref. [59]. Copyright© 2012 Elsevier Ltd. All rights reserved.

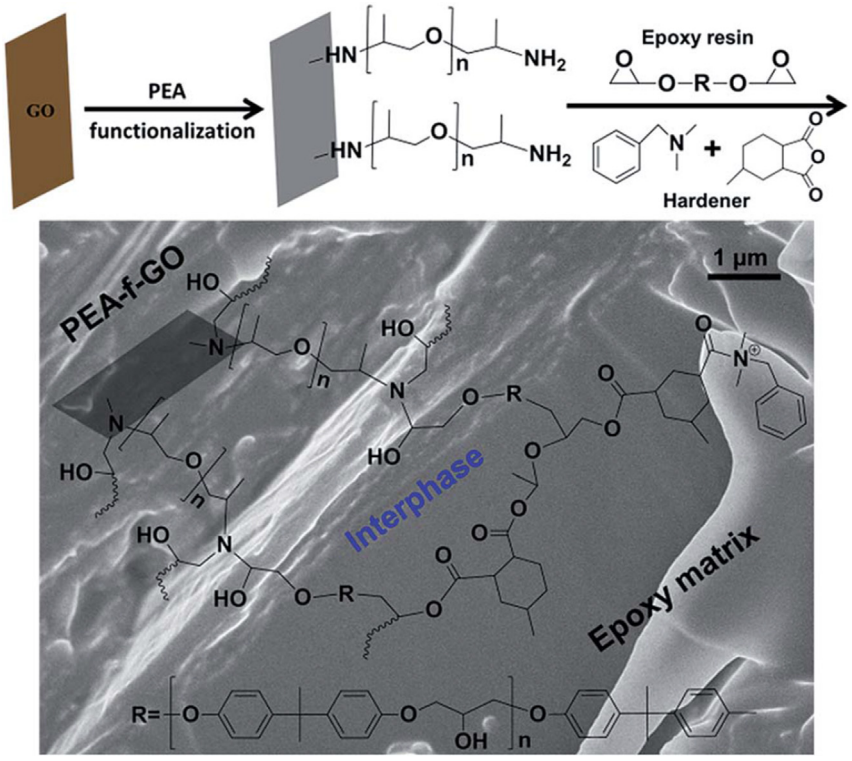

Fig. 19. Proposed PEA-functionalized-GO/epoxy nanocomposite formation mechanism. Reproduced by permission from Ref. [60]. The Royal Society of Chemistry.

interphase, because of high molecular weight, and suffered high deformation. While the lower molecular weight PEA-f-GO/epoxy composites constrained the chains movement and hence, allowed low deformation and better load transfer (as shown in Fig. 20). The shorter chains displayed better stress transfer mechanism, but low ductility and toughness.

In another approach methylenedianiline (MDA) was covalently functionalized on the surface of GO (Fig. 21) to understand the curing induced phase separation in epoxy/polyetherimide (epoxy/PEI) binary system. It was observed that GO–MDA suppressed the phase separation and arrested the morphology at an early stage. Storage modulus was observed to improve by 58.5% by the addition of 3 wt% of GO–MDA [61].

5.2. Non-covalent functionalization

This approach was quite successful in rendering uniform dispersion of CNT where in the π-electron cloud was used to harness different molecules via cation–π, π–π and CH–π type of interactions. Some of these strategies motivated researchers to

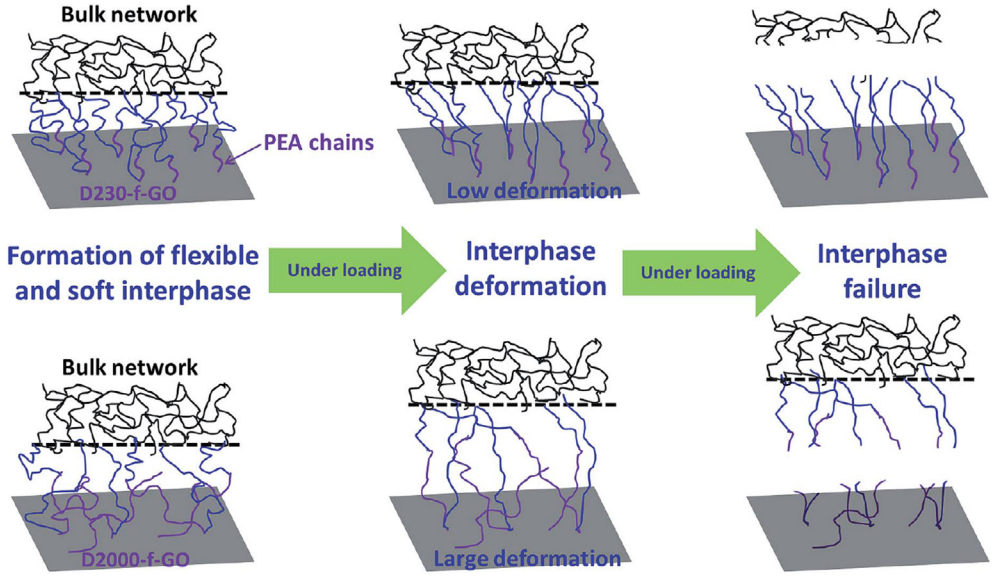

Fig. 20. Schematic of different interphase structures around GO sheets and their deformation upon loading. Reproduced by permission from Ref. [60]. The Royal Society of Chemistry.

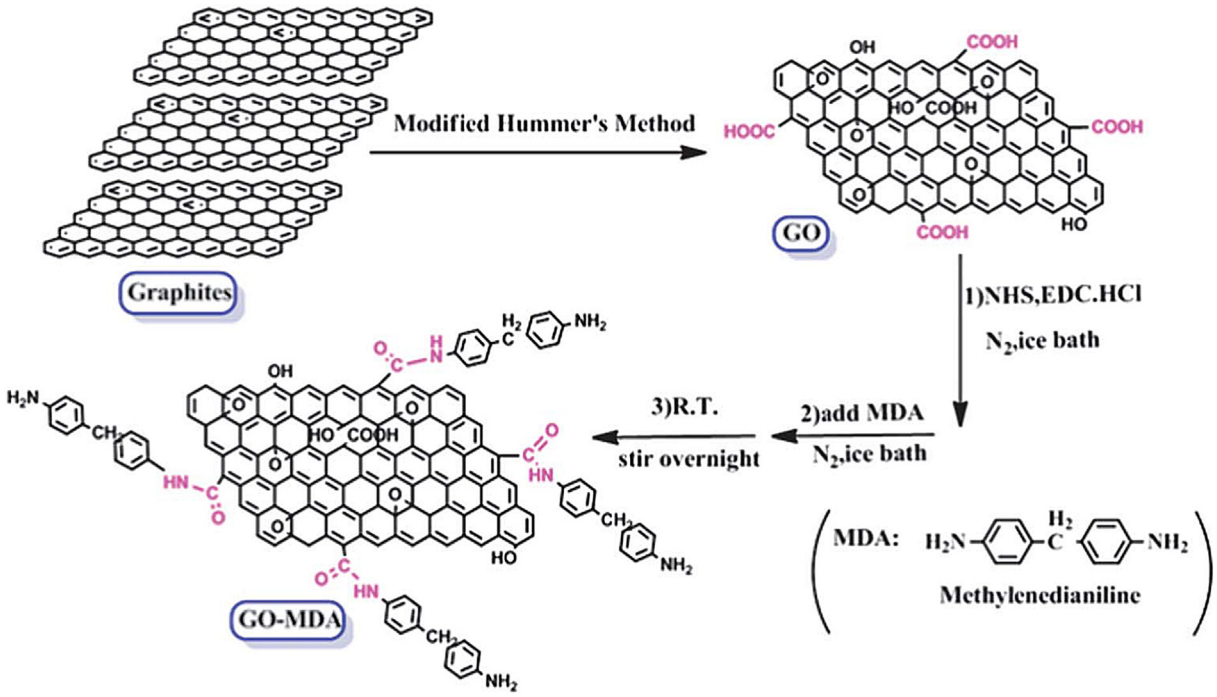

Fig. 21. Synthesis of GO and GO–MDA. Reproduced by permission from Ref. [61]. The Royal Society of Chemistry.

modify the surface of GO to improve the wettability and compatibility with epoxy resin. GO was prepared using Hummers method, and then thermally reduced in a quartz tube at 1050 °C for 30 s inside a muffle furnace. For functionalizing GO, Triton X-100 (polyoxyethyleneoctyl phenyl ether, POPE) (150 mg) was mixed with thermally reduced graphene (100 mg) in 100 mL water and sonicated at 65 °C for 6 h. During sonication process POPE was physically absorbed on the graphene sheets. The functionalized graphene was suspended in water, filtered, and dried to obtain POPE non-covalently functionalized graphene. Fig. 22 shows the TEM and AFM micrographs of functionalized graphene. From SEM micrographs (Fig. 23) of the fractured surface of composites, it was observed that Triton-graphene showed improved adhesion with the matrix. It was also evident from the broken sheets where a part of the sheet was well embedded into the matrix [62].

GO was functionalized non covalently with functional poly(glycidyl methacrylate) containing localized pyrene groups (Py-PGMA) to enhance the thermal conductivity of epoxy composites. (see Fig. 24). The thermal conductivity analysis was performed using hot disc thermal analyzer. It was found that Py-PGMA-GNS (graphene nanosheet)/epoxy composite increased the thermal conductivity by 800% compared to neat epoxy samples with addition of only 4 phr GNS. Non covalent functionalization of GNS rendered uniform dispersion and an increase in the contact area with the polymer matrix. This possibly led to enhanced phonon diffusion as argued by the authors [63].

In yet another effort to achieve superior thermal and mechanical properties of epoxy through non-covalent functionalization, 2D graphite flakes (GFs), dispersed in pyridine, were functionalized with pyrenebutyric acid (PBA), termed as f-GFs and was then dispersed into epoxy matrix to study the mechanical and thermal behavior. The storage modulus was increased by 100% relative to neat epoxy, due to fact that f-GFs provided better adhesion and compatibility with the matrix and can be attributed to interaction between carboxylic groups and epoxy, restricting molecular motion of chains. This interaction also assisted in improved phonon scattering which determines the thermal conductivity of the composites [64] Fig. 25.

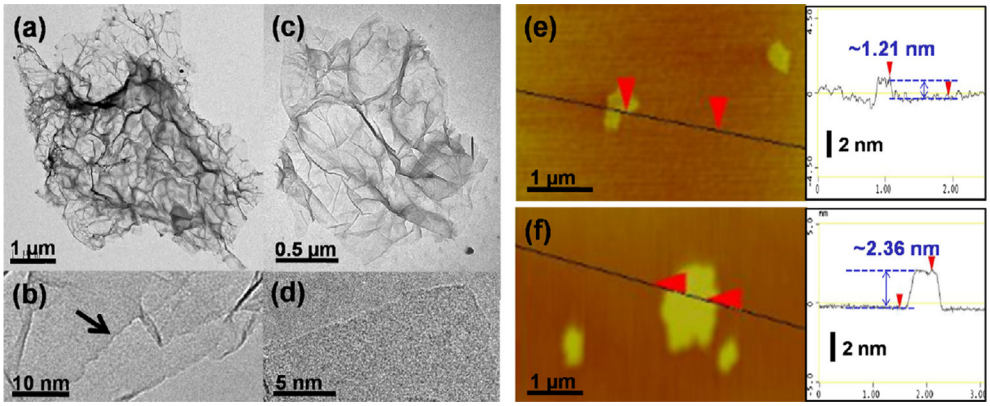

Fig. 22. Typical micrographs of (a and b) TEM images of pristine graphene; (c and d) TEM images of Triton-graphene; AFM images of (e) pristine graphene and (f) Triton-graphene deposited onto a mica substrate from an aqueous dispersion. Reproduced by permission from Ref. [62]. Copyright© 2013 Elsevier Ltd. All rights reserved.

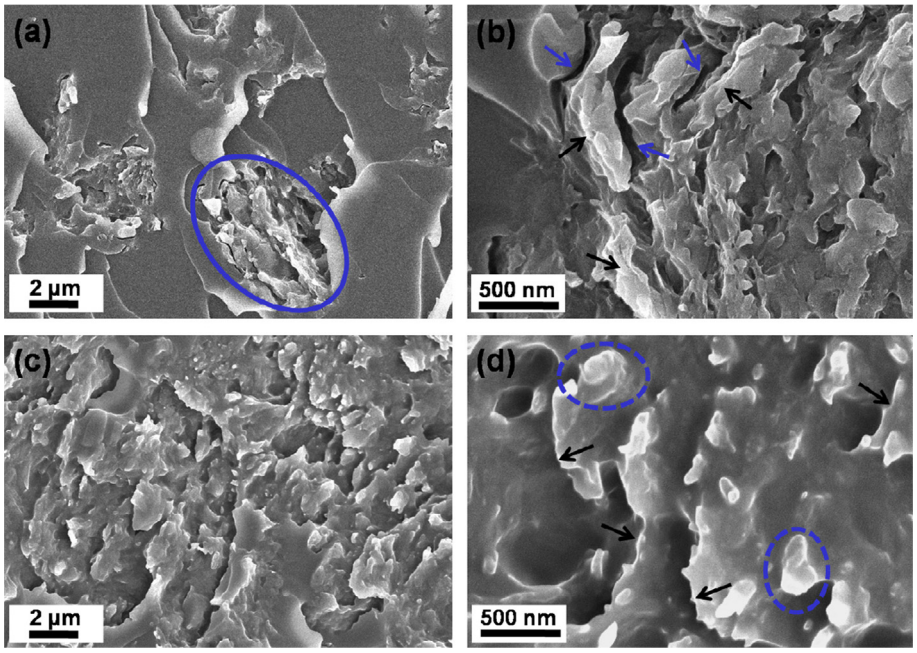

Fig. 23. SEM images of fracture surface of composite samples with 0.2 wt% graphene: (a and b) pristine graphene/epoxy, poor adhesion; (c and d) Triton-graphene/epoxy, good adhesion. Reproduced by permission from Ref. [62]. Copyright© 2013 Elsevier Ltd. All rights reserved.

6. Conclusion and outlook

In this review, our emphasis has been to highlight the importance of functionalization of graphene and its derivatives on the properties of thermoset matrix. We have briefly discussed different synthesis method and characterization techniques for graphene and its derivatives. We have also summarized different works carried out in the field graphene/epoxy nanocomposites over the decade which includes type of functionalization, processing methods (mechanical mixing, shearing, ball milling, roll milling), filler contents, mechanical, thermal and electrical properties. The covalent functionalization of graphene/graphene oxide distorted the sp^2 hybridization, unlike the non-covalent functionalization. However, the covalently functionalized graphene displayed enhanced mechanical properties, due to better interfacial bonding and efficient dispersion. Hence, it can be concluded that improved surface functionality, physical or chemical, of graphene/graphene oxide provides platform for achieving superior properties in the nanocomposites at very low levels [36,39,53,54,56,65].

After decade of scientific efforts, researchers have proposed certain potential application for functionalized graphene/epoxy composites. Surface behavior of functionalized graphene and

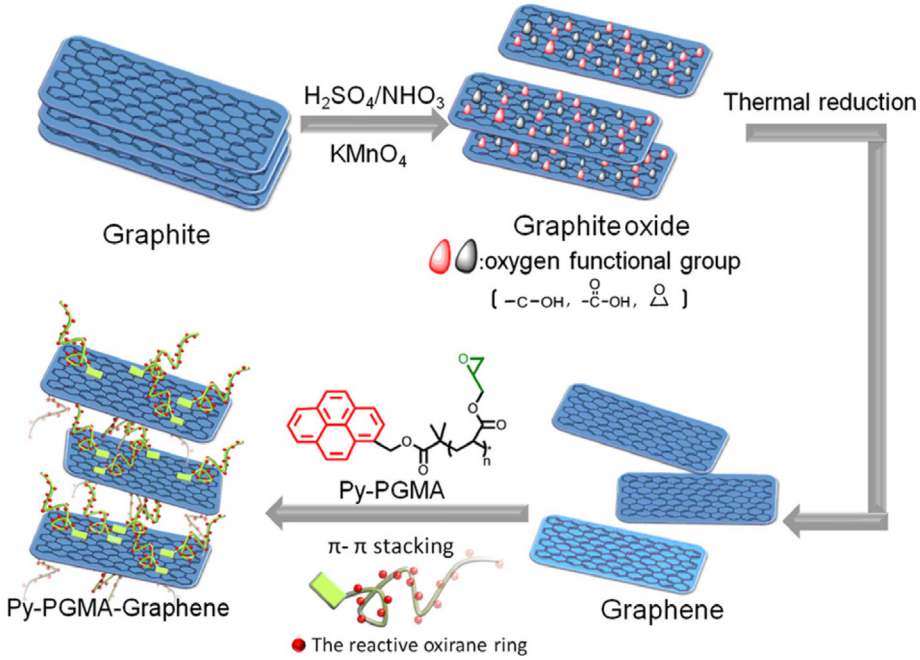

Fig. 24. Schematic representation of the preparation of graphene and functionalization of graphene. Reproduced by permission from Ref. [63]. Copyright© 2011 Elsevier Ltd. All rights reserved.

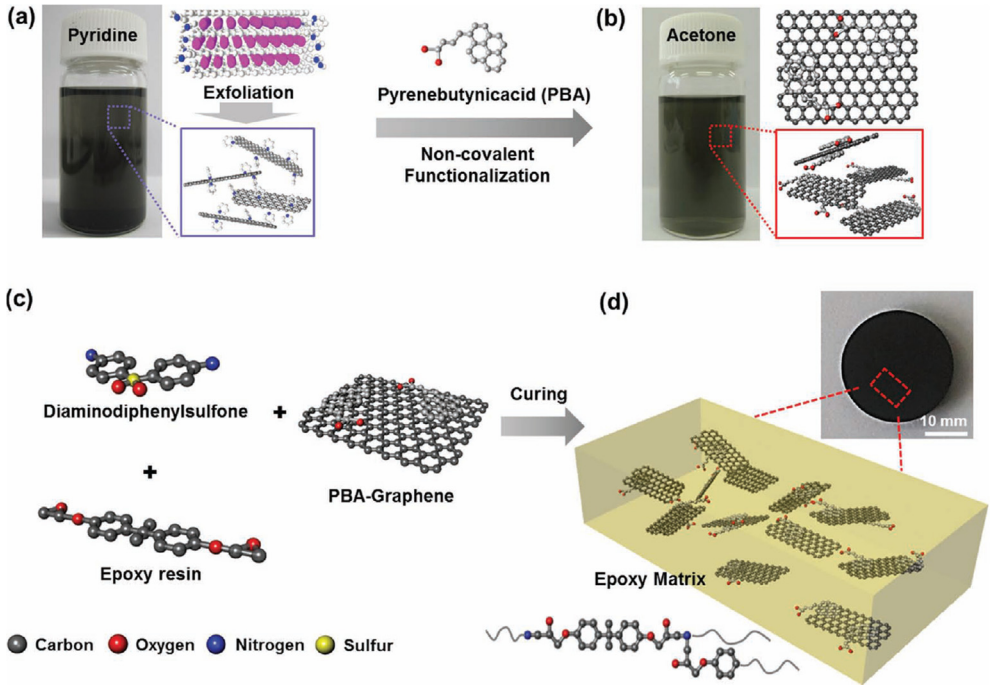

Fig. 25. Schematic diagram showing the overall processing required for the f-GFs and f-GFs-nanocomposites: a) GFs using ternary eutectic system of the alkali salts and digital photography image of dispersed f-GFs in pyridine. b) Non-covalent functionalized GFs by PBA and digital photograph image of dispersed f-GFs in acetone. c) Mixing epoxy resin, Curing Agent, and f-GFs through sonication. d) Curing process for the fabrication f-GFs-nanocomposites for 1 h at 175 °C and Digital photograph image of f-GFs–Nanocomposites. Reproduced by permission from Ref. [64]. Copyright© 2013 Wiley Ltd. All rights reserved.

related nanoparticles helps in the formation of a better interphase with matrix phase at nanoscale level hence, improves different properties and opens up new horizon of materials for different application ranging from structural, electronics, adhesives, EMI shielding, etc. For instance, graphite nanoplatelets/epoxy composites are being used as thermal interface materials given that they provide excellent thermal conductivity, low thermal resistance, better exfoliation and dispersion in the matrix phase [66]. Lee et al. [67] proposed functionalized graphene sheets/epoxy nanocomposites for cryo-tank considering its mechanical properties at sub-ambient conditions (−130 °C). Functionalized graphene incorporated in the epoxy matrix was studied for electromagnetic interference shielding applications. It was found that at filler content of 8.8 vol% the composites showed 21 dB of SE effectiveness in the frequency range of 8.2–12.4 GHz [68]. Yousefi et al. [69] proposed rGO/epoxy composites for antistatic coatings, EMI shielding and thermal conductors given its remarkable electrical and thermal behavior. $Al(OH)_3$ functionalized graphene nanosheets based epoxy composites were developed as an anisotropic conductive adhesives [57]. Microwave exfoliated reduced graphene oxide incorporated epoxy composites were observed to be a good candidate for conductive adhesives and EMI shielding applications [70].

Few areas, which we feel that should be more focused upon, are transparent coatings that can shield electromagnetic radiations like in radar applications. In addition, graphene/thermoset based composites can be explored for shape memory and self-healing applications. These areas are commercially relevant and by systematic research, practical problems associated with these areas can be addressed in a better way.

Acknowledgments

Authors would like to acknowledge Department of Science and Technology (DST), Council of Scientific and Industrial Research (CSIR), New Delhi, India.

References

[1] V. Singh, D. Joung, L. Zhai, S. Das, S.I. Khondaker, S. Seal, Prog. Mater. Sci. 56 (8) (2011) 1178–1271.
[2] T. Kuila, S. Bose, A.K. Mishra, P. Khanra, N.H. Kim, J.H. Lee, Prog. Mater. Sci. 57 (7) (2012) 1061–1105.
[3] S. Stankovich, D.A. Dikin, G.H. Dommett, K.M. Kohlhaas, E.J. Zimney, E.A. Stach, R.D. Piner, S.T. Nguyen, R.S. Ruoff, Nature 442 (7100) (2006) 282–286.
[4] Z.-S. Wu, W. Ren, L. Gao, J. Zhao, Z. Chen, B. Liu, D. Tang, B. Yu, C. Jiang, H.-M. Cheng, ACS Nano 3 (2) (2009) 411–417.
[5] M. Zhou, Y. Zhai, S. Dong, Anal. Chem. 81 (14) (2009) 5603–5613.
[6] G. Lu, L.E. Ocola, J. Chen, Nanotechnology 20 (44) (2009) article number: 445502.
[7] C. Gómez-Navarro, R.T. Weitz, A.M. Bittner, M. Scolari, A. Mews, M. Burghard, K. Kern, Nano Lett. 7 (11) (2007) 3499–3503.
[8] Y. Zhu, S. Murali, W. Cai, X. Li, J.W. Suk, J.R. Potts, R.S. Ruoff, Adv. Mater. 22 (35) (2010) 3906–3924.
[9] X. Wang, L. Zhi, K. Müllen, Nano Lett. 8 (1) (2008) 323–327.
[10] X. Miao, S. Tongay, M.K. Petterson, K. Berke, A.G. Rinzler, B.R. Appleton, A.F. Hebard, Nano Lett. 12 (6) (2012) 2745–2750.
[11] Z. Fan, J. Wang, Z. Wang, H. Ran, Y. Li, L. Niu, P. Gong, B. Liu, S. Yang, Carbon 66 (2014) 407–416.
[12] X. Sun, Z. Liu, K. Welsher, J.T. Robinson, A. Goodwin, S. Zaric, H. Dai, Nano Res. 1 (3) (2008) 203–212.
[13] A.K. Geim, K.S. Novoselov, Nat. Mater. 6 (3) (2007) 183–191.
[14] M. Lotya, Y. Hernandez, P.J. King, R.J. Smith, V. Nicolosi, L.S. Karlsson, F.M. Blighe, S. De, Z. Wang, I. McGovern, J. Am. Chem. Soc. 131 (10) (2009) 3611–3620.
[15] A.A. Green, M.C. Hersam, Nano Lett. 9 (12) (2009) 4031–4036.
[16] X. Li, W. Cai, J. An, S. Kim, J. Nah, D. Yang, R. Piner, A. Velamakanni, I. Jung, E. Tutuc, Science 324 (5932) (2009) 1312–1314.
[17] A. Reina, X. Jia, J. Ho, D. Nezich, H. Son, V. Bulovic, M.S. Dresselhaus, J. Kong, Nano Lett. 9 (1) (2008) 30–35.
[18] X. Li, X. Wang, L. Zhang, S. Lee, H. Dai, Science 319 (5867) (2008) 1229–1232.
[19] L. Jiao, L. Zhang, X. Wang, G. Diankov, H. Dai, Nature 458 (7240) (2009) 877–880.
[20] D.V. Kosynkin, A.L. Higginbotham, A. Sinitskii, J.R. Lomeda, A. Dimiev, B.K. Price, J.M. Tour, Nature 458 (7240) (2009) 872–876.
[21] D.C. Marcano, D.V. Kosynkin, J.M. Berlin, A. Sinitskii, Z. Sun, A. Slesarev, L.B. Alemany, W. Lu, J.M. Tour, ACS Nano 4 (8) (2010) 4806–4814.
[22] S. Stankovich, D.A. Dikin, R.D. Piner, K.A. Kohlhaas, A. Kleinhammes, Y. Jia, Y. Wu, S.T. Nguyen, R.S. Ruoff, Carbon 45 (7) (2007) 1558–1565.
[23] W. Chen, L. Yan, P.R. Bangal, Carbon 48 (4) (2010) 1146–1152.
[24] H. Kim, A.A. Abdala, C.W. Macosko, Macromolecules 43 (16) (2010) 6515–6530.

[25] V.C. Tung, M.J. Allen, Y. Yang, R.B. Kaner, Nat. Nanotechnol. 4 (1) (2009) 25–29.
[26] G.P. Kar, S. Biswas, S. Bose, Phys. Chem. Chem. Phys. 17 (3) (2015) 1811–1821.
[27] P.K.S. Mural, A. Banerjee, M.S. Rana, A. Shukla, B. Padmanabhan, S. Bhadra, G. Madras, S. Bose, J. Mater. Chem. A 2 (41) (2014) 17635–17648.
[28] W.-L. Song, M.-S. Cao, M.-M. Lu, S. Bi, C.-Y. Wang, J. Liu, J. Yuan, L.-Z. Fan, Carbon 66 (2014) 67–76.
[29] Z. Chen, C. Xu, C. Ma, W. Ren, H.M. Cheng, Adv. Mater. 25 (9) (2013) 1296–1300.
[30] D.-X. Yan, P.-G. Ren, H. Pang, Q. Fu, M.-B. Yang, Z.-M. Li, J. Mater. Chem. 22 (36) (2012) 18772–18774.
[31] S. Biswas, G.P. Kar, D. Arora, S. Bose, RSC Adv. 5 (31) (2015) 24132–24138.
[32] G. Vleminckx, S. Bose, J. Leys, J. Vermant, M. Wubbenhorst, A.A. Abdala, C. Macosko, P. Moldenaers, ACS Appl. Mater. Interf. 3 (8) (2011) 3172–3180.
[33] D. Wang, X. Zhang, J.-W. Zha, J. Zhao, Z.-M. Dang, G.-H. Hu, Polymer 54 (7) (2013) 1916–1922.
[34] S. Bose, T. Kuila, M.E. Uddin, N.H. Kim, A.K. Lau, J.H. Lee, Polymer 51 (25) (2010) 5921–5928.
[35] H. Pang, T. Chen, G. Zhang, B. Zeng, Z.-M. Li, Mater. Lett. 64 (20) (2010) 2226–2229.
[36] Z. Li, R. Wang, R.J. Young, L. Deng, F. Yang, L. Hao, W. Jiao, W. Liu, Polymer 54 (23) (2013) 6437–6446.
[37] X. Wang, J. Jin, M. Song, Carbon 65 (2013) 324–333.
[38] Z. Li, R.J. Young, R. Wang, F. Yang, L. Hao, W. Jiao, W. Liu, Polymer 54 (21) (2013) 5821–5829.
[39] H. Yang, C. Shan, F. Li, Q. Zhang, D. Han, L. Niu, J. Mater. Chem. 19 (46) (2009) 8856–8860.
[40] S.G. Miller, J.L. Bauer, M.J. Maryanski, P.J. Heimann, J.P. Barlow, J.-M. Gosau, R.E. Allred, Compos. Sci. Technol. 70 (7) (2010) 1120–1125.
[41] J.R. Potts, D.R. Dreyer, C.W. Bielawski, R.S. Ruoff, Polymer 52 (1) (2011) 5–25.
[42] W. Lee, J.U. Lee, B.M. Jung, J.-H. Byun, J.-W. Yi, S.-B. Lee, B.-S. Kim, Carbon 65 (2013) 296–304.
[43] T.K. Gupta, B.P. Singh, R.K. Tripathi, S.R. Dhakate, V.N. Singh, O. Panwar, R.B. Mathur, RSC Adv. 5 (22) (2015) 16921–16930.
[44] K.-H. Liao, Y.T. Park, A. Abdala, C. Macosko, Polymer 54 (17) (2013) 4555–4559.
[45] C. Bora, P. Bharali, S. Baglari, S.K. Dolui, B.K. Konwar, Compos. Sci. Technol. 87 (2013) 1–7.
[46] Z. Wang, X. Shen, M. Akbari Garakani, X. Lin, Y. Wu, X. Liu, X. Sun, J.-K. Kim, ACS Appl. Mater. Interf. 7 (9) (2015) 5538–5549.
[47] R. Shah, T. Datashvili, T. Cai, J. Wahrmund, B. Menard, K. Menard, W. Brostow, J. Perez, Mater. Res. Innovations 19 (2) (2015) 97–106.
[48] A. Joshi, A. Bajaj, R. Singh, A. Anand, P. Alegaonkar, S. Datar, Compos. Part B: Eng. 69 (2015) 472–477.
[49] M. Wang, N. Hu, L. Zhou, C. Yan, Carbon 85 (2015) 414–421.
[50] W.S. Saw, M. Mariatti, J. Mater. Sci. Mater. Electron. 23 (4) (2012) 817–824.
[51] L. Yu, J.S. Park, Y.-S. Lim, C.S. Lee, K. Shin, H.J. Moon, C.-M. Yang, Y.S. Lee, J.H. Han, Nanotechnology 24 (15) (2013) article number: 155604.
[52] S. Chatterjee, F. Nafezarefi, N. Tai, L. Schlagenhauf, F. Nüesch, B. Chu, Carbon 50 (15) (2012) 5380–5386.
[53] M. Naebe, J. Wang, A. Amini, H. Khayyam, N. Hameed, L.H. Li, Y. Chen, B. Fox, Sci. Reports (2014) 4.
[54] T. Liu, Z. Zhao, W.W. Tjiu, J. Lv, C. Wei, J. Appl. Polym. Sci. 131 (9) (2014).
[55] C. Bao, Y. Guo, L. Song, Y. Kan, X. Qian, Y. Hu, J. Mater. Chem. 21 (35) (2011) 13290–13298.
[56] T. Jiang, T. Kuila, N.H. Kim, B.-C. Ku, J.H. Lee, Compos. Sci. Technol. 79 (2013) 115–125.
[57] J. Kim, Yim B-s, Kim J-m, J. Kim, Microelectron. Reliab. 52 (3) (2012) 595–602.
[58] Y. Li, D. Pan, S. Chen, Q. Wang, G. Pan, T. Wang, Mater. Des. 47 (2013) 850–856.
[59] X. Wang, W. Xing, P. Zhang, L. Song, H. Yang, Y. Hu, Compos. Sci. Technol. 72 (6) (2012) 737–743.
[60] L.-Z. Guan, Y.-J. Wan, L.-X. Gong, D. Yan, L.-C. Tang, L.-B. Wu, J.-X. Jiang, G.-Q. Lai, J. Mater. Chem. A 2 (36) (2014) 15058–15069.
[61] G. Yu, P. Wu, Polym. Chem. 5 (1) (2013) 96–104.
[62] Y.-J. Wan, L.-C. Tang, D. Yan, L. Zhao, Y.-B. Li, L.-B. Wu, J.-X. Jiang, G.-Q. Lai, Compos. Sci. Technol. 82 (2013) 60–68.
[63] C.-C. Teng, C.-C.M. Ma, C.-H. Lu, S.-Y. Yang, S.-H. Lee, M.-C. Hsiao, M.-Y. Yen, K.-C. Chiou, T.-M. Lee, Carbon 49 (15) (2011) 5107–5116.
[64] S.H. Song, K.H. Park, B.H. Kim, Y.W. Choi, G.H. Jun, D.J. Lee, B.S. Kong, K.W. Paik, S. Jeon, Adv. Mater. 25 (5) (2013) 732–737.
[65] L. Chen, S. Chai, K. Liu, N. Ning, J. Gao, Q. Liu, F. Chen, Q. Fu, ACS Appl. Mater. Interf. 4 (8) (2012) 4398–4404.
[66] A. Yu, P. Ramesh, M.E. Itkis, E. Bekyarova, R.C. Haddon, J. Phys. Chem. C 111 (21) (2007) 7565–7569.
[67] J.K. Lee, S. Song, B. Kim, Polym. Compos. 33 (8) (2012) 1263–1273.
[68] J. Liang, Y. Wang, Y. Huang, Y. Ma, Z. Liu, J. Cai, C. Zhang, H. Gao, Y. Chen, Carbon 47 (3) (2009) 922–925.
[69] N. Yousefi, X. Lin, Q. Zheng, X. Shen, J.R. Pothnis, J. Jia, E. Zussman, J.-K. Kim, Carbon 59 (2013) 406–417.
[70] A.B. Nair, B.T. Abraham, P.S. Beegum, E.T. Thachil, Polymer 55 (16) (2014) 3614–3627.
[71] M.A. Rafiee, J. Rafiee, I. Srivastava, Z. Wang, H. Song, Z.Z. Yu, N. Koratkar, small 6 (2) (2010) 179–183.
[72] M.A. Rafiee, J. Rafiee, Z. Wang, H. Song, Z.-Z. Yu, N. Koratkar, ACS Nano 3 (12) (2009) 3884–3890.
[73] J. Jia, X. Sun, X. Lin, X. Shen, Y.-W. Mai, J.-K. Kim, ACS Nano 8 (6) (2014) 5774–5783.
[74] D. Cai, J. Jin, K. Yusoh, R. Rafiq, M. Song, Compos. Sci. Technol. 72 (6) (2012) 702–707.
[75] T. Jiang, T. Kuila, N.H. Kim, J.H. Lee, J. Mater. Chem. A 2 (27) (2014) 10557–10567.
[76] D. Galpaya, M. Wang, G. George, N. Motta, E. Waclawik, C. Yan, J. Appl. Phys. 116 (5) (2014) 053518.
[77] C. Liu, Z. Wang, Huang Ya, H. Xie, Z. Liu, Y. Chen, W. Lei, L. Hu, Y. Zhou, R. Cheng, RSC Adv. 3 (44) (2013) 22380–22388.
[78] X.-J. Shen, X.-Q. Pei, S.-Y. Fu, K. Friedrich, Polymer 54 (3) (2013) 1234–1242.
[79] K. Liu, L. Chen, Y. Chen, J. Wu, W. Zhang, F. Chen, Q. Fu, J. Mater. Chem. 21 (24) (2011) 8612–8617.
[80] Z. Tang, H. Kang, Z. Shen, B. Guo, L. Zhang, D. Jia, Macromolecules 45 (8) (2012) 3444–3451.
[81] S. Chatterjee, J. Wang, W. Kuo, N. Tai, C. Salzmann, W. Li, R. Hollertz, F. Nüesch, B. Chu, Chem. Phys. Lett. 531 (2012) 6–10.
[82] A. Yasmin, J.-J. Luo, I.M. Daniel, Compos. Sci. Technol. 66 (9) (2006) 1182–1189.
[83] D.R. Bortz, E.G. Heras, I. Martin-Gullon, Macromolecules 45 (1) (2011) 238–245.

Suryasarathi Bose is currently an Assistant Professor at the Indian Institute of Science (IISc), Bangalore, India. He received his Ph.D. degree from Indian Institute of Technology (IIT), Bombay, India in 2008. For a brief period, he worked as a research associate at IIT Bombay before he joined Prof. Paula Moldenaers's group in Katholieke University of Leuven (Belgium) as a postdoctoral researcher. His research interests include polymer blends, self-assembly of nanomaterials using phase separation in polymer blends as tool, carbon nanotubes and graphene based polymer nanocomposites, rheology and structure-property correlations in homopolymers and blends.

Rani Rohini is currently pursuing her PhD under Dr. Suryasarathi Bose in the Department of Materials Engineering, Indian Institute of Science, Bangalore, India. She completed her Bachelor in Polymer Engineering from Pune University in the year 2012. Her research interest includes functionalization of graphene oxide, carbon nanotubes and carbon fiber based epoxy nanocomposites.

Prajakta Prathamkumar Katti is pursuing her Ph.D in Materials Engineering Department, Indian Institute of Science, Bangalore under the supervision of Dr. Suryasarathi Bose. She completed her bachelor's degree from Pune University in 2011. She received her Master's degree from Pune University in 2014. Her current research includes epoxy-PEEK composites.